HOKKAIDO UNIVERSITY

Title	Mapping the change of coral reefs using remote sensing and in situ measurements: a case study in Pangkajene and Kepulauan Regency, Spermonde Archipelago, Indonesia
Author(s)	Haya, La Ode Muhammad Yasir; Fujii, Masahiko
Citation	Journal of oceanography, 73(5), 623-645 https://doi.org/10.1007/s10872-017-0422-4
Issue Date	2017-10
Doc URL	https://hdl.handle.net/2115/71562
Rights	The final publication is available at Springer via http://dx.doi.org/10.1007/s10872-017-0422-4
Type	journal article
File Information	Manuscript JOOC.pdf

Hokkaido University Collection of Scholarly and Academic Papers : HUSCAP

Mapping the Change of Coral Reefs Using Remote Sensing and *in situ* Measurements; A Case Study in PANGKEP Regency, Spermonde Archipelago, Indonesia

La Ode Muhammad Yasir Haya[1, 2], Masahiko Fujii[1]

[1]*Graduate School of Environmental Science, Hokkaido University, N10 W5, Kita-Ku Sapporo, Hokkaido 060-0810, Japan.*

[2]*Marine Science Department, Faculty of Fisheries and Marine Science, Halu Oleo University, Jln. HEA. Mokodompit Kendari, 93232, Southeast Sulawesi, Indonesia*

Tel.: +81-11-706-3026

Fax: +81-11-706-2359

Abstract: As elsewhere in Indonesia, Local inhabitants in the Pangkajene and Kepulauan (PANGKEP) Regency, Spermonde Archipelago area and along the south-west coast of Sulawesi traditionally regard the coral reefs as their livelihood source. Since human activities as well as natural disturbances posed major threats to the coral reefs, these livelihoods may also be at risk. Currently, no comprehensive information on the status and condition of coral reefs in this area is available for this resource management. We determined the changes of coral reef habitat over a period of 20 years from 1994 to 2014 using a satellite Landsat multi-temporal image substantiated with *in-situ* measurement data collected in 2014. The spectral value of coral reefs was extracted from multi-temporal Landsat imagery data, while the diffuse attenuation coefficient of water was obtained by using statistical analysis between the ratio of live coral cover and the spectral value of the visible bands. By using the unsupervised classification integrated with the data ground truth, it is stated that there has been a decline in live coral cover over a period of 20 years from 7,716 ha in 1994 to 4,236 ha in 2014, with a degradation rate of 174 ha/yr. Based on the results, the ratio of the coral cover in the coral reef transects varied from the average of 24% for live corals to 96% for coral rubbles, implying the degraded status of coral reefs in the study area.

Keywords: *coral reefs, depth invariant index (DII), multi-temporal Landsat, remote sensing*

✉ La Ode Muhammad Yasir Haya

yasir.haya@ees.hokudai.ac.jp

Introduction

Coral reefs have been exploited as resources for income, fisheries, construction materials, tourism and recreational and other purposes for thousands of years (Hodgson 1999; McManus 1997; Mumby and Steneck 2008). Ecologically, coral reefs fulfill an important role in maintaining the balance of marine resource productivity and serve as indicators of the health of the marine environment (Hourigan et al. 1988; Hein et al. 2015).

In recent decades, changes in coral reef ecosystems have occurred on both regional and global scales due to natural effects and anthropogenic factors (Burke et al. 2011; Wilkinson 2008). Burke et al. (2011) reported that more than 60% of the world's coral reefs were threatened directly by one or multiple factors, including overfishing, destructive fishing, coastal development, and environmental pollution. Among these, overfishing and destructive fishing were the most widely practiced, affecting more than 55% of the world's coral reefs (Bruno and Selig 2007; Burke et al. 2011). Furthermore, on a regional scale, the threat of coral reefs occur in the Coral Triangles. Coral Triangles, lying in Indonesia, the Philippines, Malaysia, Timor-Leste, Papua New Guinea and the Solomon Islands, are the world's center of marine biodiversity, particularly coral reefs (World Wild Fund-WWF 2016).

Since 1998, the Indonesian Government has paid significant attention to manage coral reef ecosystem through the Coral Reef Rehabilitation and Management Program (COREMAP). The purpose of this program is protection, rehabilitation and management focused on the sustainable use of coral reefs and related marine ecosystems in Indonesia, which in turn will support the welfare of coastal communities (World Bank 2015). Unfortunately, in some locations, COREMAP has been insignificantly reducing coral reef exploitation activities, especially in areas outside COREMAP sites. Fishing activities that threaten coral reef ecosystems continued to be practiced inside some COREMAP locations, such as Pangkajene and Kepulauan (PANGKEP) Regency in Spermonde Archipelago, South Sulawesi. The large size of the area and limited resources (equipment and coral reef data) were considered as major obstacles in monitoring and protecting the coral reefs. Up-to-date information is essential for designing an effective policy and management systems to protect coral reefs. One of the methods that could be used to fill this gap is the use of remote sensing technology.

Remote sensing technology has several advantages over other technologies in terms of providing multi-year databases so that only periodic coral reef field monitoring is necessary (Goodman et al. 2013; Mumby and Harborne 1999). Remote sensing can be effectively used to determine the status of coral reefs, and has been used by researchers

for scientific investigation, management, and mapping. Roelfsema et al. (2002) used Landsat Thematic Mapper (TM) imagery to study the spatial distribution of microalgae in coral reefs. Lubin et al. (2001) measured coral reef and non-coral reef reflectance using a coupled ocean–atmosphere radiative transfer model and showed that various spectral features could be used to distinguish coral reefs from the surroundings. The data used as input are generally obtained from surface or aircraft data, although aircraft data are generally obscured in terms of spectral measurements. Lubin et al. (2001) support the conclusion of recent research that the use of satellite remote sensing is effective for coral reef mapping. Although detailed reef mapping (e.g., species identification) is difficult, Mumby (2001) developed an explicit method to chart coral species distribution.

The combination of remote sensing and *in situ* data can be used to verify the evolution of coral reef degradation, including its recovery over timescales of years to decades. Scopélitis et al. (2009) identified the typology of coral reef communities using remote sensing data combined with integrated *in situ* data between 1973 and 2003 in Saint-Leu Reef in the Indian Ocean. Five aerial photographs and two QuickBird images combined with field observations were used to detect the changes in coral reefs during three impact periods, two caused by storms in 1989 and 2002, and one by coral reef bleaching in 2002. Scopélitis et al. (2009) concluded that there was no significant change in the patchy reefs

between 1973 and 2006 due to the rapid recovery rate of corals (*Acropora* Sp.) from bleaching. Palandro et al. (2008) quantified coral reef degradation in Florida Keys Natural Marine Sanctuary, USA, from 1984 to 2002, using Landsat imagery and determined the coral reef destruction to be 61%, or 3.4% /yr. Using different generations of Landsat imagery, i.e. Landsat 5 TM (1987), Landsat 7 ETM (2000), and Landsat 8 OLI (2013), with field observation data from 2004, El-Askary et al. (2014) detected changes in coral reefs in Hurgadha, Egypt. Using supervised classification, changes in coral reef habitats can be identified qualitatively and quantitatively for specific periods.

Similar studies have been conducted in Indonesia. Nurdin et al. (2015) have studied changes in the coral reefs of the coastal area of a small island (Suranti Island) in the PANGKEP Regency by using multi-temporal Landsat imagery as their primary data source. However, there are no previous studies that have focused on changes in the coral reefs of all the islands over the PANGKEP Regency.

Additionally, this study was not only used the data from the multi-temporal Landsat imagery (from the year of 1994 to 2014), but also the in-situ data of the coral reef habitats monitoring. Purkis and Pasterkamp (2004) reported that the integration of these data will provide advantages in terms of accuracy, time, cost-effectiveness and coverage area (Jupiter et al. 2013; Hedley et al. 2016; Mumby et al. 1999; Mumby et al. 2004).

Considering these conditions, to elucidate changes in coral conditions and the causes in the PANGKEP Regency, it is considered important to analyze large-scale data as well as limitation of data availability in this area. Therefore, this study aimed to provide a map of the coral reefs distribution around the area, identify and calculate the changes in the ratio of coral cover in two decades from 1994 to 2014.

Materials and Methods

Study Site

The study was carried out in the PANGKEP Islands, Spermonde Archipelago, South Sulawesi Province, Indonesia (Fig.1). Geographically, the sites were situated within 118^{o}54’36”E - 119^{o}35’24”E and 4^{o}30’36”S - 5^{o}03’48”S. Administratively, there are 41 islands (including 31 islands inhabited) that consist of two districts of Liukang Tuppabiring and Tuppabiring Utara (Statistics Indonesia of Pangkajene and Kepulauan Regency 2014). Along the coastal area from Makassar City to the PANGKEP Regency, there are six rivers and five of them are active rivers all the year around. Ecologically, corals in the Spermonde Archipelago including those in the PANGKEP Regency are

classified into four ecological zones (Hoeksema 2012), namely inner zone that contains muddy sand as a bottom substrate, followed by middle inner zone which contains many coral islands, middle outer zone of which coral reef areas are still submerged, and outer zone as a barrier reef zone which contains coral islands (Fig. 1).

Since 1994, 50,000 ha of the outer islands in the PANGKEP Regency have been designated as marine protected areas (MPAs) by decree of the Minister of Forestry No. 588/Kpts-VI/1996 and the decree of the Minister of Marine and Fisheries No. 66/MEN/2009 (Fig. 1). In addition, this site is within the COREMAP location which was implemented from 2004 to 2010. Since then, the exploitation and use of coral reefs have been restricted to ensure the sustainable management.

Data Sources

Satellite Landsat Imagery Data

We used Landsat 5 Thematic Mapper (TM), Landsat 7 Enhanced Thematic Mapper (ETM), and Landsat 8 Operational Land Imager (OLI) multi-temporal imagery, acquired in 1994, 2002, and 2014, respectively. The analysis of changes in the coral reefs was performed for a 20-year period, considering the ability of coral reefs to recover from stress

conditions occurring within this period (Wilkinson 2008). The types and characteristics of the Landsat image are summarized in Table 1.

The study area was covered in the same scene in Landsat 5 TM and 7 ETM (path/row: 114/63), whereas Landsat 8 OLI covered the area in two scenes (path/row: 114/63 and 115/63). The Landsat data had a spatial resolution of 30 m. The Landsat image acquired in 2002 was chosen to minimize the loss of information due to incomplete data caused by technical problems during data acquisition. Moreover, the data obtained before Scan Line Corrector (SLC) turned-off selection were recommended by NASA's Millennium Coral Reef Mapping Project (NASA 2009).

Data of Coral Reef Condition

In-situ data of coral reef condition were collected using the point intercept transect (PIT) method (Hill and Wilkinson 2004). The locations for PIT survey were chosen to represent Hutchinson's ecological zone of the Spermonde Archipelago (Hoeksema 2012), i.e., inner zone (Saugi and Karanrang Islands), middle-inner zone (Badi and Sanane Islands), middle-outer zone (Samatellu and Sarappo Islands), and outer zone (Tambakulu, Gondongbali, Pandangan, and Kapoposang Islands), as can be seen in Fig. 1. Transect points were chosen based on the coral distribution area around the coastline. A 50-m

transect line was set above the coral reefs at 3-10 m depth, parallel to the coastline. The position of each transect line (coordinate point) was taken using a global positioning system (GPS), type of Garmin/eTrex Vista HCx. Technically, the point coordinates were taken exactly at the centerline of the transect. The objects along the line were observed and documented. In the PIT method, objects over the transect line were recorded at a 0.5 m spacing.

In order to evaluate the condition of the coral reefs, all categories in the PIT method (Fig. 2) were further classified as shown in Table 2. Live coral cover (%) was calculated to evaluate the condition of coral reefs as proposed by Gomez and Yap (1988):

$$\text{Live coral cover } (\%) = \frac{\text{Each component}}{\text{Total component}} \times 100, \qquad (1)$$

Based on the percentage of live coral cover, the condition was classified from “bad” to “excellent” (Table 3) according to Gomez and Yap (1988). The percentage of coral rubble can be regarded as an indicator of coral reef damage caused by destructive fishing (Jameson et al. 1999). In addition to live coral cover, the coral mortality index (MI) was also used to evaluate the coral reef condition (Gomez et al. 1994):

$$\mathrm{MI} = \frac{\text{Ratio of dead coral (\%)}}{\text{Ratio of live coral (\%)} + \text{Ratio of dead coral (\%)}}, \qquad (2)$$

In-situ Ground Control Point and Ground Truth Data

In addition to the in-situ data obtained by the PIT method, the ground control point (GCP) and ground truth (GT) coordinate points were determined using a global positioning system (GPS), type of Garmin/eTrex Vista HCx. Generally, the GCP points were road intersections, docks, or other landmarks identifiable in the satellite images. Ground truth data were obtained using GPS for each type of seabed cover, including live corals, dead corals, sea-grasses, and sand. In addition, the GT data were applied to check the accuracy of the image classification results.

Social Survey Data

In order to ensure the results of primary data analysis, social survey was conducted to obtain complemental information about fishing activities in the coral reef area, i.e. fishing location, fishing gear used, destructive fishing activities and so on. In the case of social survey, questionnaires were distributed to the fishermen and their households following Krejcie and Morgan (1970)'s method. Based on the population size on ten

inhabited islands, 296 fishermen were chosen as respondents through purposive random sampling.

Secondary Data

We used a PANGKEP regional administration map (1:250,000) and Indonesia coastal environmental map (1:250,000) obtained from the Government of PANGKEP Regency to identify the islands and bathymetry in the study area.

Image Processing

In this study, the image processing was carried out in the areas not affected by turbidity and sedimentation because the sensor is only able to penetrate the turbidity of the water at a depth of less than 1 m. Based on Hutchinson's ecological zone, reef areas analyzed include middle inner zone, outer middle zone, and the outer zone (Hoeksema 2012). Image processing consisted of several phases as follows:

Atmospheric Correction

Scattering and absorption of molecules by the atmosphere decreases the quality of information in the satellite image by up to 10%, depending on the spectral channel (Che and Price 1992; Ishizaka et al. 1992). Therefore, an atmospheric correction is essential in order to minimize the effect of the atmosphere in multi-temporal images before comparing and analyzing the data (Hadjimitsis et al. 2010). In this study, an atmospheric correction was applied to the three series of Landsat imagery data using Dark Object Subtraction 1 (DOS1) Method (Chavez 1996). For easier atmospheric correction, we applied semi-automatic classification plugin (SCP) in QGIS version 2.10 (Congedo and Macchi 2013).

Geometric Correction

Geometric correction for Landsat 5 TM and Landsat 7 ETM imagery data was conducted using the same GCPs on Landsat 8 OLI corrected as a reference. This aims to improve the accuracy and minimize the geometric error in Landsat imagery data. Eight GCPs were chosen for the geometric correction using order polynomial transformation and the nearest neighbor interpolation algorithm (Baboo and Devi 2011). The corrected

image is acceptable if the root mean square error (RMSE) is a one-half pixel wide (RMSE = 0.5). Overall, the RMSE less than 0.5 pixel were achieved for each transformation.

Mosaic Image

Mosaicking is a process to merge two or more scenes into a single scene or image. The process was applied to Landsat 8 OLI imagery data since in this Landsat image, the study area (PANGKEP in the Spermonde Archipelago) was captured in two scenes (path/row: 114/63 and 115/63). This is in contrast to previous Landsat imagery data that require only one scene (path/row: 114/63). Since 2010, Landsat 8 OLI has replaced previous Landsat versions such as Landsat 7 ETM and Landsat 5 TM. In the mosaicking process, the digital value of both images needs to be balanced and normalized by using smooth intensity filter modulation (SFIM) pan sharpen wizard of ER Mapper in order to increase the spectral qualities of merged images (ERDAS 2008).

Subset Image (Cropping)

Creating a subset image, or "cropping," aims to delimit the area of interest, reinforce geospatial phenomenon, and focus on the study area. In addition, the subset image

produces objects that are larger in size, allowing existing information such as color to be seen more clearly.

Image Composite (True Color)

True color on Landsat 5 TM and Landsat 7 ETM was displayed by using combination bands of Red: Green: Blue (R: G: B) 3: 2: 1, whereas the color was displayed as R: G: B = 4: 3: 2 on the Landsat 8 Operational Land Imager (OLI). This band combination is often used to detect feature types covering shallow bottom waters in the preliminary stage. Chlorophyll in vegetation were detected using green canal (band 2 in Landsat 5 TM and Landsat 7 ETM, and band 3 in Landsat 8 OLI).

High chlorophyll concentration on the mainland provided a high digital reflection value and was shown as dark green. Water bodies were detected using band 1 (Landsat 5 TM and 7 ETM) and band 2 (Landsat 8 OLI) in the blue composite so that water bodies could be depicted in blue.

Total Suspended Matter

One of the controlling factors for the growth of coral reefs is the total suspended matter (TSM) concentration in the coastal water. The threshold of the TSM concentration for normal coral reef growth is 10 mg/L (Erftemeijer et al. 2012). The growth of coral reefs is considered lower if the concentration is higher than the threshold. Further, too-high TSM concentrations prevent from detection by the Landsat satellite. Light intensity exponentially decreases with the water depth, due to light absorption and scattering by water molecules, suspended particles and soluble materials (e.g., Weinberg 1976; Falkowski et al. 1990). In such a condition, the detection capacity of the Landsat satellite could be less than 1 m depth.

On the other hand, the TSM concentrations in coastal waters can be estimated from the Landsat image using near infra-red (NIR) band, by using an algorithm of Zheng et al. (2015), as described in the following functions:

$$TSM_{OLI} = 6110.3 \times R_{rs}(NIR) - 1.8242, \qquad (3)$$

$$TSM_{TM/ETM} = 4616.4 \times R_{rs}(NIR) - 4.362, \qquad (4)$$

where TSM_{OLI} is the total suspended matter for Landsat 8 OLI (mg/L), $TSM_{TM/ETM}$ is the total suspended matter for Landsat 5 TM or 7 ETM (mg/L), R_{rs} (NIR) is the NIR band reflectance (λ) , which is Band 5 for the Landsat 8 OLI sensor and Band 4 for the Landsat 5 TM or 7ETM sensors. The areas in which the concentration of TSM is higher than 10 (mg/L) were excluded for further analysis in this study because of the poor detection capacity of the Landsat satellite with high TSM concentration and light attenuation. In this case, coral reefs in the bottom waters were not able to be detected by the Landsat sensor.

Water Column Correction

Correction of the water column was done to improve image quality by reducing the interference in the water column. The technique commonly used for the correction of the water column is based on an algorithm developed by Lyzenga (1978; 1981). The radiance measurements were performed on the same type bottom substrate with different depth so that the radiance values of band *i* and band *j* are correlated linearly. By using statistical analysis, a gradient value of the linear line equation was an approximation of the attenuation coefficient between band *i* and band *j* which is formed by two pair bands

between red, green and blue bands (Research Center for Oceanography-Indonesian Institute of Sciences 2014). The equation is written as follows (Green et al. 2000):

$$\text{Depth invariant index } = \text{Ln}(Li) - \left[\left(\frac{ki}{kj}\right) \times \text{Ln}(Lj)\right], \qquad (5)$$

where Li and Lj are the radiance after atmospheric correction for band i and band j respectively, and $\frac{ki}{kj}$ is the ratio of the diffuse attenuation coefficients of band i and j.

Unsupervised Classification, Reclassification and Ground Truthing

An unsupervised classification was performed using image-processing software (ER Mapper 7.2) and the three depth-invariant bands derived from the Lyzenga model. Unsupervised classification algorithms identify natural groups within multi-spectral data (Call et al. 2003). Iterative Self-organizing Class Analysis (ISOCLASS) was used for the classification. Image-processing software were automatically classifies spectral value into spectral classes (Lillesand et al. 2004). Then we simply match objects on the field with the help of global positioning system (GPS). In this case, 30 unlabeled classes with 150 iterations were produced from images, which included water column correction. After that, reclassification was applied to the results of the unsupervised classification

image based on visual interpretation (spectral class color) and digital image value. Interpretation of the digital image value was carried out using the cell value profile tools of the ER Mapper 7.2 (ERDAS 2008) and the visual interpretation (Table 4) referred to the COREMAP image interpretation guide (COREMAP 2001, cited in Suwargana 2014).

Based on the results, shallow features could be classified into five categories: sea, live corals, dead corals, sea-grasses, and sand. The results of the classification were then verified using field data (243 points) to obtain the level of accuracy of mapping.

Accuracy Assessment

Accuracy assessment is closely related to the position and thematic accuracy (Congalton and Green 2008), which is done by using a confusion matrix. This method compares the image obtained from classification results as the basis for the actual class with field data, which are assumed to represent the seabed cover (Campbell 1987; Call et al. 2003). Data row are obtained by remote sensing data classification, which signify the accuracy calculation by the producer, while the data column is a calculation result of field observations by researchers and used in user's accuracy calculation (Table 5). More consistencies between classification and observation results would generate higher

overall accuracy, which is calculated using the following equation (Congalton and Green 2008):

$$Overall\ accuracy = \frac{\sum_{i=1}^{k} N_{ij}}{N} \times 100\%, \quad (6)$$

$$Producer\ accuracy\ j = \frac{N_{jj}}{N_{+j}} \times 100\%, \quad (7)$$

$$User\ accuracy\ i = \frac{N_{ii}}{N_{i+}} \times 100\%. \quad (8)$$

Not all agreement can be attributed to the success of the classification. Therefore, the Kappa analysis were also performed to assess the extent of classification accuracy as that accounts for not only diagonal elements but all the elements in the confusion matrix (Campbell 1987; Call et al. 2003). The Kappa analysis is a multivariate technique analysis used to calculate the discrete value of classification accuracy of the confusion matrix, and is done by evaluating the Kappa value, calculated by the following equation (Green et al. 2000):

$$Kappa = \frac{N\sum_{i=1}^{k} N_{ij} - \sum_{i=1}^{k} N_{i+}\, N_{+j}}{N^2 - \sum_{i=1}^{k} N_{i+}\, N_{+j}}, \quad (9)$$

where N_{ij} is the number of observation at column j and row i, N_{ii} *and* N_{jj} are the numbers of observation categorized as the thematic class of i and j, respectively, N_{i+} and N_{j+} are the numbers of observation classified as the thematic class of i from satellite data and that of j from in-situ data, and N is the total number of observations.

The Kappa value would be lower than the value of overall accuracy and it has a range between 0 and 1. Based on several previous studies, the Kappa analysis is one of the methods to validate the result of image classification (Campbell 1987; Call et al. 2003; Green et al 2000; Lillesand et al. 2014). In order to interpret the Kappa value, we refer to the Fleiss interpretation (1969) that categorized as follows: > 0.75 as “very good”, 0.40-0.75 as “fair” to “good”, and <0.4 as “bad”.

Vectorization

The image classification results were converted into vector data formats. This approach had three objectives: to manipulate the data in the image, to remove disturbance (e.g., ocean surface wave movement and turbidity of the water), and to map the

distribution and condition of the coral reefs and conduct an analysis of changes in the reefs.

Post-classification

In this stage, we produced maps of the coral reef distribution and condition based on the extracted Landsat multi-temporal imagery data. We produced three maps, one each for 1994, 2002, and 2014 when the images were acquired. We also generated maps of the changes in coral reef condition over a 20-year period obtained by overlaying the map of coral reef change between 1994 and 2002 with the map of coral reef change from 2002 to 2014.

All stages of the data processing and analysis in this study are shown in Fig. 3.

Results

Status of Coral Reefs

The physical status of coral reefs was expressed in the classification system by calculating the ratio of the certain coral coverage area. The common method used to

determine the physical status of coral reefs is the Point Intercept Transect (PIT) (Hill and Wilkinson 2004). Our observations of coral reef condition in 2014 using the PIT method in ten locations (nine inhabited islands and one uninhabited island) are shown in Fig.4 and Table 6.

Table 6 indicated that among the total stations consisted of 23 stations observed in this study, five stations of coral reefs exhibited good physical condition, two stations were in moderate physical condition, and sixteen stations showed bad physical condition, respectively.

The mean live coral cover percentage was 24%, and the mean percentage of the dead coral cover was 62%, although the percentage differed significantly among transects. These values reveal that the condition of the coral reefs in the study area was relatively bad. Furthermore, the coral mortality index (MI) was 0.75, which is classified as severely damaged. Coral reefs classified as bad or severely damaged are considered to negatively affect the coral reef ecosystem, including species abundance and diversity (Jones et al. 2004; Komyakova et al. 2013).

Components of rubbles on the coral reefs (coral rubbles) can be indicators to identify the activity of destructive fishing because of the physical damage to coral reefs in the form of wreckages or rubbles commonly caused by the use of bombs on fishing (Jameson

et al. 1999). Based on the result, coral rubble in the study area had the highest percentage of coverage relative to the other components, as can be seen in Fig. 5.

The percentage of coral rubble varied among transects, with a mean of 95.8%. The lowest percentage was found at Saugi Island (87.8%), and the highest occurred at Badi Island and Kapoposang Island (both 100%). The high ratio of coral rubbles in the study area indicates that most of the coral reef damages are derived from destructive fishing practices, i.e. blast fishing and cyanide fishing.

Location of destructive fishing practices in the study area were related to the distance from settlements and post-supervision. Remote areas are often difficult to be monitored by supervisory officers and local communities. Based on a calculation using "Plugin Distance between Points of Quantum Geographic Information System (QGIS)", there was a relationship between the distance from the mainland and the number of fishermen that like to choose remote locations to catch reef fishes in a year (before and in 2014) (Table 7).

The islands located close to the mainland generally had a lower frequency of coral fish catching compared to the islands located farther from the mainland. Based on the result, it is found that especially, the coral reefs located farther from the mainland or remote areas, i.e. Kapoposang MPAs, Langkai, Lanyukang, Suranti, Jangang-Jangangang

Islands, are used as favorite locations of destructive fishing practices using bombs and cyanide.

In this study, correlation test were examined by using statistical analysis to know how relationship between the distance of fishing location and the amount of respondent to choose a favorite fishing location. The result of the correlation analysis, it shows that there is a positive correlation between the distance of fishing location and the amount of respondent to choose a favorite fishing location with a coefficient correlation (r) was 0.68 (in 2014) and 0.75 (before 2014).

The characteristics of the fishing locations obtained from the questionnaire survey showed four types of locations preferred by fishermen (Fig. 6). The respondents' preferences were deep sea/offshore (44%), reef flat (22%), reef edge (19%), and coastal water (15%). The high ratio of preferences for deep sea/offshore is considered to be resulting from that the area is the main target for fishermen using large vessels. Some of the fishermen set artificial fishing grounds (locally known as "*rumpon*") and use small bombs to herd fish into the nets. In contrast, based on the result, flat and edge reefs (totally 41%) are considered to be preferred for blast and cyanide fishing which were strongly linked to the fishing gears used and target fish species frequently caught.

Image Processing

A geometric correction process was performed using eight GCPs, which resulted in average RMSE of 0.5 for Landsat images. Atmospheric correction were conducted to the three series Landsat imagery data. Based on the result, profile spectral shows the spectral reflectance at sea surface after atmospheric correction on Landsat image, within visible bands with central wavelength range of 0.485 through 0.660 μm (blue, green and red bands). The pattern in shorter wavelength of Landsat 8 OLI is different from Landsat 5 TM and Landsat 7 ETM, as shown in Fig. 7.

Visually, the objects in terms of reflectance in descending order are sand, seagrasses, dead corals and live corals. This result agrees with a previous result by Luczkovich et al. (1993) which reported higher reflectance of sand than sea-grasses and coral reefs. It is clearly demonstrated that the atmosphere correction improves the visible band, hence it is possible to differentiate each object. This shows that the Landsat image with spatial resolution 30 m can be used as an input in the analysis to detect the change of coral reef covering a wide area. Landsat image offers advantages not only in detecting and mapping coral reef geomorphology and underwater habitat but also in being freely available and updated periodically. Therefore, it was extensively used previously by several previous

studies (e.g., El-Askary et al. 2014; Hedley et al. 2016; Kordi and O'Leary 2016; Palandro et al. 2008; Roelfsema et al. 2002; Wahiddin et al. 2015).

Total Suspended Matter Detection

Sensor Landsat has the capability to identify total suspended matter (TSM) in the water by using band near infra-red (NIR). TSM is the optical properties of a suspension that causes light to be scattered and absorbed rather than transmitted through the water column (Davies-Colley and Smith 2001) and it became a limiting factor for the growth of coral reefs (Parwati et al. 2013; Zheng et al. 2015). Distribution of the TSM concentration in around inner zone areas can be evidence directly in the field where there are six rivers estuary, i.e. Tello, Maros, Pangkajene, Labakkang, Limbangan, and Segeri, along with the coastal areas from Makassar to the PANGKEP Regency (Fig.8). They are as a supplier of sediment materials to the sea water.

Based on the image processing, the TSM concentration in the inner zone are <10-120 (mg/L), <10-186 (mg/L), and <10-203 (mg/L) for Landsat 5 TM (1994), Landsat 7 ETM (2002) and Landsat 8 OLI (2014), respectively. Higher TSM concentrations are found around river mouths, while lower TSM concentrations are generally found in areas further from the mainland. Fig. 8 demonstrates that the TSM concentration and

distribution area have increased from 1994-2002 to 2002-2014 periods. This trend is possibly caused by several factors, e.g. land use activities (Tonasa Cement Factory in the PANGKEP Regency and Bosowa Cement Factory in the Maros Regency), rainfall and oceanographic factors in the coastal area.

High TSM concentration affects coral reef growth by decreasing the sunlight penetration and further hinders the photosynthesis. The threshold of TSM concentration for normal coral reef growth is 10 mg/L (Erftemeijer et al. 2012). Coral reef growth is considered to be lower with higher TSM concentration than the threshold. In the inner zone, therefore, the TSM concentration generally exceeds the threshold, which implies that the coral reef growth is disturbed and coral reef ecosystem and its sustainability are threatened.

To avoid possible biases in change in coral cover, the area of the inner zone (coastal water nearby the mainland) was excluded in the analysis. Therefore, for further analysis, we focused on middle inner through outer zones.

Water Column Correction

The percentage of live coral cover in the PIT method used to estimate the spectral live coral cover per pixel. Technically, the coordinates of the transect observation of coral

plotted into the image and then carried out extraction pixel value by point on the bands visible (i.e., blue, green and red) to obtain the pixel value of the coral reefs at each transect observation. After that, these spectral values of the tree series Landsat images were calculated by using statistical analysis to obtain the gradient coefficient of the ratio of two pair bands as the ratio of the diffuse attenuation coefficient (ki/kj) (Fig. 9).

The spectral values of live coral reefs are distributed around the linear line in particular on the band ratio of blue and green bands (Fig. 9 (a, (d), (g)). Distribution of spectral value with the ratio of two pair bands of blue and green look fairly consistent on three series of Landsat imagery data according to determination coefficient of Landsat 5 TM, 1994 (0.90), Landsat 7 ETM, 2002 (0.98) and Landsat 8 OLI, 2014 (0.92). Because the ratio of the diffuse attenuation coefficient is stable for combination of radiance (L) at blue and green wavelengths in live coral reefs, they are detectable by using L at two wavelengths.

The values of the gradient of the linear line (k_i/k_j) at each Landsat imagery were applied to the three series of Landsat imagery data to obtain new images. Results of the water column correction are shown in the Fig. 10.

Based on the result shows that the object of the live corals, dead corals, sea-grass and sand can be distinguished visually by color and spectral values. Grouping the spectral

value is done by the image processing program. A cluster of spectral with the cyan color is interpreted as corals and seems to dominate in the three series of Landsat imagery, while in the class of dead coral, shown as cluster of green color is also widespread especially on Landsat 8 OLI, 2014.

Unsupervised Classification, Reclassification and Ground Truthing

In this stage, data of multi-temporal Landsat images resulted from water column correction especially in ratio of the blue and green band were used as input in the unsupervised classification process. Utilization of blue and green band for this classification due to the energy from spectrum of band blue and band green can penetrate deeper to the water column compare to the other band.

The results of unsupervised classification were obtained several categories with each category represents underwater objects. Furthermore, the process of identification and classification of the coral reefs and seabed habitats was done based on the guidelines COREMAP (See Table 3 for the classification).

In addition, the field survey data were set as references in reclassification phase, which after adjustment it was produced 4 classes of dominant covers underwater: live corals, dead corals, sea-grasses and sand. The grouping from 30 to 4 classes was backed

by field survey data. In this case, different unlabelled classes with the same object were combined into one class. After that, these classes were done reclassification to be 4 classes (Table 8 and Fig. 11).

The result of the images classification on multi-temporal Landsat imagery of data (i.e., Landsat 8 OLI, 2014, Landsat 7 ETM, 2002, and Landsat 5 TM, 1994) (Table 8), shows that the class of live corals is a class with the highest percentage of 58.33 % (209,301 pixels), followed by dead corals amounted to 23.70% (85,049 pixels), sand 10.51% (37,712 pixels) and the lowest is sea-grasses at 7.46% (26,754 pixels).

In 1994, the areas were 7,716 ha, 1,128 ha, 838 ha, and 1,082 ha for live coral, dead coral, seagrass, and sand, respectively, which implies a low percentage of damaged coral reefs (10.48%) compared to live corals (71.68%). A high percentage of live coral offers advantages in terms of ecology and economic security for local people in this area. The coral reef distribution, including its condition based on analysis of the 1994 Landsat image, is shown in Fig. 11 (a). The pattern of live coral distribution (in cyan) can be clearly seen in all zones, although some red spots indicating dead corals are also observed. Red spots can be clearly observed in the outer zone, which includes the Kapoposang Marine Conservation Area. This area comprises Kapoposang, Pandangan, Tambakulu, Gondongbali, and Suranti Islands.

In 2002, Live corals were still visible and distributed in all of the study sites, although red spots had begun to appear in some coral reefs, especially in the northern part of the outer-middle to outer zone, such as Suranti Island and Jangang-Jangangang coral clusters, and also in the southern part of the outer zone, such as Lanjukang Island and coral clusters. In the middle-inner zone, dead corals had also begun to appear, but the area was still dominated by live coral. In this period, coral reef damage was more severe in the outer zone compared to the middle-outer and middle-inner zones (Fig. 11 (b)). Overall, the coral life was reduced by 7.72 % and dead coral increased by 10.05%.

In 2014, the percentage of dead corals increased by 19.56%, or about 4.316 ha. Contrasting with dead coral, the percentage of live corals in this period decreased by 24.6% or about 4,326 ha. As can be seen in the Fig. 11 (c), distribution of dead coral clearly visible red and spread, not only in the area of coral reefs within the outer zone but also in the middle inner zone.

Accuracy Assessment

After designed the map of coral reef physical condition through the interpretation of satellite images, the next step was accuracy test. An accuracy test was performed on the classification result of the Landsat 8 OLI image based on the field data obtained in 2014

for four habitat classes (live corals, dead corals, sand, and sea-grasses) which aims to validate the correctness and proper of measurement and it could be used for further analysis. Points for accuracy test taken as many as 243 points which are scattered throughout the study area, and is considered to represent any characteristics of the object in the field. The field data were then used to construct the error matrix (Tables 9 and 10). Based on the data analyses of the error matrix, the individual and overall accuracy was expressed in percentage value (%).

The precision of classification is calculated using overall accuracy of the confusion matrix, which in this case field survey data is set as a reference in validation. Confusion matrix also produces value producer accuracy (PA) and user accuracy (UA). The results in Table 6 shows that 198 of 243 points are correctly classified and OA accuracy value obtained is 81.48%. According to Lillesand et al. (2014), interpretation result was considered good if it has accuracy higher than 80%. Therefore, the level of accuracy in this study is considered good.

Furthermore, the Kappa value was calculated based on confusion matrix to validate the result of classification. The level of Kappa value was determined by the image resolution and image processing techniques. Similarly, the distribution of random points based on the density of each category in the ground truth data (i.e. proportionate stratified

samples) would lower the value of errors. In this case, the Kappa value of 0.77 indicates that the pixels were more correctly classified by 77% than would be expected by chance alone.

PA value is the value of each pixel on a proper class, which had been classified. The biggest value of PA cover seabed habitats found on dead corals (87.87%), which is correctly classified and omission error of 12.13%. Omission error value is to remove areas that should be included in the class (Boschetti et al. 2004). The smallest PA value is found in sand (77.41%) with omission error 22.59% (Table 10).

UA value is the average probability of actual pixels representing each class in the field. In Table 10, dead corals (84.05%), which is correctly classified and error commission value of 15.95 % represents the largest UA values. Commission error is an error in mapping according to the class, which includes areas that should be removed from the class (Boschetti et al. 2004). The smallest UA value is both sea-grasses and sand with the percentages of 80% respectively, which is also correctly classified and the value of each commission error of 20%.

Based on the accuracy test, there was a bias between image interpretation results and the actual data in the field, which was contributed by several factors such as water condition and error in field data collection. During image acquisition, different objects at

the bottom of the waters with almost identical spectral reflectance would cause similar appearance in the image. Another factor is a human error caused by the observer during data acquisition in the field. During the survey, agitated and wavy water condition made the sampling at planned coordinate difficult to execute.

Change in Coral Reefs Habitat

In this study, it was demonstrated that depth invariant index algorithm could be applied to multi-temporal Landsat imagery data in order to extract information of objects existing in shallow water. Validation by in-situ data in classification stage was a key factor in determining mapping accuracy of 81.48%. Based on the result, the Landsat multi-temporal images of 1994, 2002, and 2014 showed that the coral reefs have changed over the 20-year period from 1994 to 2014 with different trends, i.e., a decline in live corals and increase in dead corals. The statistics for the changes in coral reef habitats from 1994 to 2014 are shown in Table 11. The results of the 2002 Landsat 7 ETM image classification show a drastic change in the live and dead coral categories. Live corals area decreased significantly, by 10.8%, from 7,716 ha in 1994 to 6,885 ha in 2002 (Fig. 12 (a)). In contrast, the dead corals area doubled, from 1,128 ha to 2,210 ha, during the same

period. The area of sea-grasses underwent a slight increase by 8 ha, whereas the sandy area decreased significantly from 1,082 ha in 1994 to 1,023 ha in 2002.

Most of the damage to the coral reefs has occurred recently, between 2002 and 2014. The coral reef condition and its distribution based on the Landsat 8 imagery data from 2014 is depicted visually in Fig. 12 (b). It can be clearly observed that dead corals (in red) is dominant compared to the other categories. There is a marked change in live coral cover, which decreased by 38.5% from 6,885 ha in 2002 to 4,236 ha in 2014, in contrast to the dead coral cover, which doubled from 2,210 ha in 2002 to 4,316 ha in 2014 **(**Fig. 12 (b)). There was an increase in the area of sea-grasses, from 846 ha in 2002 to 906 ha in 2014, and the sandy area increased significantly, from 1,023 ha in 2002 to 1,306 ha in 2014.

In addition, the results of the Landsat image multi-temporal classification and spatial analysis show that the area of live corals decreased by 45.1% from 7,716 ha in 1994 to 6,885 ha in 2002, and then declined dramatically to 4,236 ha in 2014; thus, over the last 20 years, the area of live corals has decreased by 3,480, or 174 ha/yr.

The changes in the coral reefs during the last 20 years are summarized in Fig. 13. From 1994 to 2014, 45.1% of the coral cover underwent change. The total change comprised changes from live to dead corals (91.6%), dead corals to sand (7.2%), and live

corals to sand (1.2%). The large change from live to dead corals implies the influence of anthropogenic activities, which cause damage and high mortality of coral reefs.

Discussion

Base on the results, the application of the water column correction using gradient of the ratio of two pair bands and unsupervised classification to the three series of Landsat imagery data (from 1994, 2002, and 2014) were effective in extracting information on four habitat classes (live corals, dead corals, sand, and sea-grasses) in shallow water. It was relatively straightforward to differentiate the four classes based on color and spectral values. All classes generated by image classification and field survey indicated that the approach could be applied effectively in mapping. This was supported by the high overall accuracy of 81.48% and Kappa value of 0.77, which means that the mapping precision is considered good.

The analysis to detect changes in coral reefs habitat based on multi-temporal imagery data revealed a significant change during the two decades from 1994 to 2014. A dramatic change occurred in live and dead coral cover, whereas there were no significant changes

in the sand and sea-grasses cover. Although changes were detected at all sites, marked changes occurred in the middle-outer zone and outer zone, which are located farthest from the mainland (Fig. 12).

On average, live corals and dead corals covered 24% and 62% of the total area, respectively; these values were classified as bad and severely damaged, respectively (Gomez and Yap 1988; Gomez et al. 1994). This finding suggests that the two methods of coral reef classification (Landsat image classification and PIT method) can be used effectively to determine the state of degradation of coral reefs.

Physical factors, i.e. current, wave and wind affect the distribution of the TSM in the study area (Jones et al. 2016). The analysis of Landsat satellite images show that the TSM can be transported to the coral reefs of the islands, which are adjacent to the inner middle zone (Fig. 8).

By contrast in the inner zone, change in coral reefs from the middle to the outer zone for the last 20 years (from 1994 to 2014) are affected by fishing activity. Based on the result, the coral reefs in the study area dominated by coral rubble. This is indicating that the cause of coral reef decline was predominantly destructive fishing practices such as blast fishing and cyanide fishing. This is evidenced by the results obtained from the PIT method, which showed a mean coral rubble cover of 95.8%, as shown in Fig.5. The other

evidence is that more than 40% of the fishing locations in the study area are in the area of coral reefs (reef flat and reef edge), as shown in Fig. 6. Our findings are in accordance with the results of previous studies (DFW-Indonesia 2003; Edinger et al. 1998; Pet-Soede 2000).

Besides the influences of TSM concentration, the ability of satellite sensors to record marine object is influenced by oceanographic factors, e.g., tides which varied daily due to the moon and the sun gravitational forces. The tidal graph of Spermonde Archipelago waters obtained from the NAO 99b Tidal Prediction System (http://www.miz.nao.ac.jp/staffs/nao99/index_En.html), as shown in Fig. 14. The graph shows the curve of tidal taken in accordance with the recording time of images. The images were recorded in 1994, 2002, 2014 (path/row: 114/63) and 2014 (path/row: 115/63) respectively at 13:27, 13:59, 14:10, and 14:17 local time.

Based on the Fig. 14, between 13:00 and 14:00 (recording time of 4 scenes), the water level on 21 Sept 2014 and 28 Sept.2014 was over 1 m, while on July 10, 2002, and August 29, 1994, the water level was below 1 m. Thus, the graph shows that the sea level varied, which depends on the recording time.

Tides is one of the parameters affecting sea level would determine the depth of water column. Differences in the depth of the sea water, in turn, will influence the results of

image analysis since the maximum depth penetration sensor of Landsat satellite is only 10 m (Nurdin et al. 2013).

Conclusions

Integration of multi-temporal Landsat imagery data and in-situ field data were used to map distribution of coral reefs and to assess changes in coral reef habitats in wide area of the PANGKEP Regency, Spermonde Archipelago, Indonesia. Our multi-temporal Landsat imagery analysis suggests that the coral reef habitats in the PANGKEP Regency, have changed drastically over the 20 years from 1994 to 2014, with a rate of coral reef destruction of 174 ha/yr. The coral reef decline in the study area is presumably caused by destructive fishing practices. The coral reef degradation is also considered to be caused by high total suspended matter concentration which hampers the growth, especially in the inner zone (nearby the mainland).

We predict that coral reef cover will continue to decrease if no protection appropriate procedures and management strategies for the coral reefs are implemented in the area,

and would very much like to call for the strategies in the study area based on the scientific insights.

Acknowledgments: The lead author is grateful to the Indonesia Endowment Fund for Education Scholarship (LPDP), Ministry of Finance of Indonesia for funding of this research. This study was conducted under the framework of the Precise Impact Assessments on Climate Change of the Program for Risk Information on Climate Change (SOUSEI Program) supported by the Ministry of Education, Culture, Sports, Science, and Technology in Japan (MEXT).

Author Contributions: La Ode Muhammad Yasir Haya was the primary analyst, author, and correspondence of author for this work. Masahiko Fujii contributed as a supervisor and revising of the paper.

Conflicts of Interest: The authors declare no conflict of interest.

Certification of proofreading: The English in this document has been checked by at least two professional editors, both native speakers of English. For a certificate, please see: http://www.textcheck.com/certificate/o3oKr7

References

Baboo SS, Devi MR (2011) Geometric correction in recent high resolution satellite imagery: a case study in Coimbatore, Tamil Nadu. International Journal of Computer Applications 14:32-37

Boschetti L, Flasse SP, Brivio PA (2004) Analysis of the conflict between omission and commission in low spatial resolution dichotomic thematic products: The Pareto Boundary. Remote Sensing of Environment 91:280-292

Bruno JF, Selig ER (2007) Regional Decline of Coral Cover in the Indo-Pacific: Timing, Extent, and Sub regional Comparisons. PLoS ONE 2:e711

Burke L, Reytar K, Spalding M, Perry A (2011) Reefs at risk revisited. World resources Institute, Washington DC, pp 130

Call KA, Hardy JT, Wallin DO (2003) Coral reef habitat discrimination using multivariate spectral analysis and satellite remote sensing. International Journal of Remote Sensing 24:2627-2639

Campbell J (1987) Introduction to Remote Sensing. Guilford Press, New York, pp 551

Chavez PS (1996) Image-based atmospheric corrections-revisited and improved. Photogrammetric engineering and remote sensing 62:1025-1035

Che N, Price J (1992) Survey of radiometric calibration results and methods for visible and near infrared channels of NOAA-7,-9, and-11 AVHRRs. Remote sensing of environment 41:19-27

Congalton RG, Green K (2008) Assessing the accuracy of remotely sensed data: principles and practices. CRC press, Taylor & Francis group, New York pp 210

Congedo L, Macchi S (2013) Investigating the Relationship between Land Cover and Vulnerability to Climate Change in Dar Es Salaam. Working Paper, pp 58

Davies-Colley R, Smith D (2001) Turbidity, suspended sediment and water quality: a review. J. Am. Water Works Assoc 37:1085–1101

DFW-Indonesia (2003) Profile of Destructive Fishing in Spermonde Islands. http://dfw.or.id/wp-content/uploads/2011/publikasi/DF_REPORT_SPERMONDE.pdf. Accessed 2 May 2014 (**in Bahasa**)

Edinger EN, Jompa J, Limmon GV, Widjatmoko W, Risk MJ (1998) Reef degradation and coral biodiversity in Indonesia: effects of land-based pollution, destructive fishing practices and changes over time. Marine Pollution Bulletin 36:617-630

El-Askary H, Abd El-Mawla S, Li J, El-Hattab M, El-Raey M (2014) Change detection of coral reef habitat using Landsat-5 TM, Landsat 7 ETM+, and Landsat 8 OLI data in the Red Sea (Hurghada, Egypt). International Journal of Remote Sensing 35:2327-2346

ERDAS (2008) ER Mapper User's Guide. ERDAS Inc., United State of America, pp.278

Erftemeijer PL, Riegl B, Hoeksema BW, Todd PA (2012) Environmental impacts of dredging and other sediment disturbances on corals: a review. Marine Pollution Bulletin 64:1737-1765

Falkowski PG, Jokiel PL, Kinzie RA (1990) Irradiance and corals. In: Dubinsky Z (eds) Ecosystems of the World 25: Coral Reefs. Elsevier, Amsterdam, pp 89-107

Fleiss JL, Cohen J, Everitt BS (1969) Large sample standard errors of kappa and weighted kappa. Psychological Bulletin 72: 323–327. doi:10.1037/h0028106

Gomez E, Yap HT (1988) Monitoring reef condition. In: Kenchington RA, Hudson BET (eds) Coral Reef Management Handbook. UNESCO Regional Office for Science and Technology for Southeast Asia (ROSTSEA), Jakarta, pp 171-178

Gomez ED, Alino PM, Yap HT, Licuanan WY (1994) A review of the status of Philippine reefs. Marine Pollution Bulletin 29: 62-68

Goodman JA, Purkis SJ, Phinn SR (2013) Coral reef remote sensing: A guide for mapping, monitoring and management. Springer Science & Business Media, USA, pp 446

Green EP, Mumby PJ, Edwards AJ, Clark CD (2000) Remote sensing handbook for tropical coastal management. UNESCO Publishing, Paris, pp 328

Hadjimitsis DG, Papadavid G, Agapiou A, Themistocleous K, Hadjimitsis MG, Retalis A, Michaelides S, Chrysoulakis N, Toulios L, Clayton CR (2010) Atmospheric correction for satellite remotely sensed data intended for agricultural applications: impact on vegetation indices. Natural Hazards and Earth System Sciences 10:89-95

Hedley JD, Roelfsema CM, Chollett I, Harborne AR, Heron SF, Weeks S, Skirving WJ, Strong AE, Eakin CM, Christensen TR, Ticzon V (2016) Remote sensing of coral reefs for monitoring and management: A review. Remote Sensing 8:118:1-40

Hein MY, Lamb JB, Scott C, Willis BL (2015) Assessing baseline levels of coral health in a newly established marine protected area in a global scuba diving hotspot. Marine environmental research 103:56-65

Hill J, Wilkinson C (2004) Methods for ecological monitoring of coral reefs. Australian Institute of Marine Science, Townsville, pp 117

Hodgson G (1999) A global assessment of human effects on coral reefs. Marine Pollution Bulletin 38:345-355

Hoeksema BW (2012) Distribution patterns of mushroom corals (Scleractinia: Fungiidae) across the Spermonde Shelf, South Sulawesi. Raffles Bull Zool 60:183-212

Hourigan TF, Tricas TC, Reese ES (1988) Coral reef fishes as indicators of environmental stress in coral reefs. Marine organisms as indicators 1988:107-135

Ishizaka J, Fukushima H, Kishino M, Saino T, Takahashi M (1992) Phytoplankton pigment distribution in regional upwelling around the Izu Peninsula detected by coastal zone color scanner on May 1982. Journal of Oceanography 48:305-327

Jameson SC, Ammar M, Saadalla E, Mostafa HM, Riegl B (1999) A coral damage index and its application to diving sites in the Egyptian Red Sea. Coral Reefs 18:333-339

Jones GP, McCormick MI, Srinivasan M, Eagle JV (2004) Coral decline threatens fish biodiversity in marine reserves. Proceedings of the National Academy of Sciences of the United States of America 101:8251-8253

Jones R, Bessell-Browne P, Fisher R, Klonowski W, Slivkoff M (2016) Assessing the impacts of sediments from dredging on corals. Marine pollution bulletin 102:9-29

Jupiter S, Roelfsema CM, Phinn SR (2013) Science and Management. In: Goodman JA, Purkis SJ, Phinn SR (eds) Coral Reef Remote Sensing A Guide for Mapping, Monitoring and Management. Springer, London, pp 403-427

Komyakova V, Munday PL, Jones GP (2013) Relative importance of coral cover, habitat complexity and diversity in determining the structure of reef fish communities. PloS one 8:1-12

Kordi, O'Leary (2016) A spatial approach to improve coastal bioregion management of the north Western Australia. Ocean & Coastal Management 127:26-42

Krejcie RV, Morgan DW (1970) Table for determining sample size from a given population. Educational and Psychological Measurement 30:607-610

Lillesand T, Kiefer RW, Chipman J (2004) Remote sensing and image interpretation. John Willey &Sons Inc., New York, pp 812

Lillesand T, Kiefer RW, Chipman J (2014) Remote sensing and image interpretation. John Wiley & Sons Inc., pp 146

Lubin D, Li W, Dustan P, Mazel CH, Stamnes K (2001) Spectral signatures of coral reefs: Features from space. Remote sensing of environment 75:127-137

Luczkovich JJ, Wagner TW, Michalek JL, Stoffle RW (1993) Discrimination of coral reefs, seagrass meadows, and sand bottom types from space: A Dominician Republic Case Study. Photogrametric Engineering & Remote Sensing 59:385-389

Lyzenga DR (1978) Passive remote sensing techniques for mapping water depth and bottom features. Applied optics 17:379-383

Lyzenga DR (1981) Remote sensing of bottom reflectance and water attenuation parameters in shallow water using aircraft and Landsat data. International Journal of Remote Sensing 2:71-82

McManus JW (1997) Tropical marine fisheries and the future of coral reefs: a brief review with emphasis on Southeast Asia. Coral Reefs 16:121-127

Mumby P, Green E, Edwards A, Clark C (1999) The cost-effectiveness of remote sensing for tropical coastal resources assessment and management. Journal of Environmental Management 55:157-166

Mumby PJ (2001) Beta and habitat diversity in marine systems: a new approach to measurement, scaling and interpretation. Oecologia 128:274-280

Mumby PJ, Harborne AR (1999) Development of a systematic classification scheme of marine habitats to facilitate regional management and mapping of Caribbean coral reefs. Biological Conservation 88:155-163

Mumby PJ, Hedley J, Chisholm JRM, Clark CD, Ripley H, Jaubert J (2004) The cover of living and dead corals from airborne remote sensing. Coral Reefs 23:171-183

Mumby PJ, Steneck RS (2008) Coral reef management and conservation in light of rapidly evolving ecological paradigms. Trends in ecology & evolution 23:555-563

NAO 99b Tidal Prediction System. http://www.miz.nao.ac.jp/staffs/nao99/index_En.html. Accessed 10 October 2016

NASA (2009) Millennium Reef Maps Metadata Updated 11 March 2009 For Landsat images. http://oceancolor.gsfc.nasa.gov/LANDSAT/HTML/README.html. Accessed 1 September 2014

Nurdin N, Prasyad H, AS MA (2013) Dinamika Spasial Terumbu Karang pada Perairan Dangkal Menggunakan Citra Landsat Di Pulau Langkai, Kepulauan Spermonde. Jurnal Ilmiah Geomatika 19:83-89 (**in Bahasa with English abstract**)

Nurdin N, Komatsu T, AS MA, Djalil AR, Amri K (2015) Multisensor and multitemporal data from Landsat images to detect damage to coral reefs, small islands in the Spermonde archipelago, Indonesia. Ocean Science Journal 50:317-325

Palandro DA, Andréfouët S, Hu C, Hallock P, Müller-Karger FE, Dustan P, Callahan MK, Kranenburg C, Beaver CR (2008) Quantification of two decades of shallow-water coral reef habitat decline in the Florida Keys National Marine Sanctuary using Landsat data (1984–2002). Remote sensing of environment 112:3388-3399

Parwati E, Kartasasmita M, Soewardi K, Kusumastanto T, Nurjaya IW (2013) The relationship between total suspended solid (TSS) and coral reef growth (case study of Derawan Island, Delta Berau Waters). International Journal of Remote Sensing and Earth Sciences (IJReSES) 10:104-113

Pet-Soede C (2000) Options for co-management of an Indonesian coastal fishery. Dissertation, Wegenigen University, see http://library.wur.nl/WebQuery/wurpubs/fulltext/121232

Purkis SJ, Pasterkamp R (2004) Integrating in situ reef-top reflectance spectra with Landsat TM imagery to aid shallow-tropical benthic habitat mapping. Coral Reefs 23:5-20

Research Center for Oceanography, Indonesian Institute of Sciences (2014) Handbook of shallow water habitats mapping. http://www.coremap.or.id/downloads/gis_1435730309.pdf. Accessed 30 September 2016 (**in Bahasa**)

Roelfsema C, Phinn S, Dennison W (2002) Spatial distribution of benthic microalgae on coral reefs determined by remote sensing. Coral Reefs 21:264-274

Scopélitis J, Andréfouët S, Phinn S, Chabanet P, Naim O, Tourrand C, Done T (2009) Changes of coral communities over 35 years: Integrating in situ and remote-sensing data on Saint-Leu Reef (la Réunion, Indian Ocean). Estuarine, Coastal and Shelf Science 84:342-352

Statistics Indonesia of Pangkajene and Kepulauan Regency (2015) https://pangkepkab.bps.go.id. Accessed 20 December 2016

Suwargana N (2014) Analysis of Alos AVNIR-2 imagery for coral reefs mapping (A Case Study: Banyuputih, Situbondo). Proceedings of the National Seminar on remote sensing, Indonesian National Institute of Aeronautics and Space (LAPAN). http://sinasinderaja.lapan.go.id/wp-content/uploads/2014/06/bukuprosiding_588-596.pdf. Accessed 10 October 2014 (**in Bahasa with English abstract**)

US Geological Survey-USGS (2014) Data sets. https://earthexplorer.usgs.gov/. Accessed on 20 December 2014

Wahiddin N, Siregar VP, Nababan B, Jaya I, Wouthuyzen S (2015) Change detection of coral reef habitat using Landsat imagery in Morotai Island North Maluku Province. Jurnal Ilmu dan Teknologi Kelautan Tropis 6:507-524 (**in Bahasa with English abstract**)

Weinberg S (1976) Submarine daylight and ecology. Marine Biology 37:291-304

Wilkinson C (2008) Status of Coral Reefs of the World: 2008 Global Coral Reef Monitoring Network and Reef and Rainforest Research Center. Townsville, Australia, pp 296

World Bank (2015) World Bank Supports Indonesia's Coral Reefs and Coastal Communities. http://www.worldbank.org/en/news/press-release/2014/02/21/world-bank-indonesia-coral-reefs-coastal-communities. Accessed 15 July 2015

World wild fund-WWF (2016) Coral Triangle. http://www.worldwildlife.org/places/coral-triangle. Accessed 20 December 2016

Zheng Z, Li Y, Guo Y, Xu Y, Liu G, Du C (2015) Landsat-Based Long-Term Monitoring of Total Suspended Matter Concentration Pattern Change in the Wet Season for Dongting Lake, China. Remote Sensing 7:13975-13999

Table 1 Types and characteristics of Landsat images used in this study. Multi-temporal Landsat imagery data were obtained from the US Geological Survey-USGS (2014)

Satellite and sensor	Acquisition date	Path/row	Spatial Resolution (m)	Acquisition time (UTC+08:00)
Landsat 5 TM	August 29, 1994	114/63	30	13:27:27
Landsat 7 ETM	July 10, 2002	114/63	30	13:59:17
Landsat 8 OLI	September 21, 2014	114/63	30	14:10:42
	September 28, 2014	115/63	30	14:17:05

Table 2. Classification of benthos in the PIT method

Classes	Description
Live coral (LC)	Acropora and non-Acropora
Dead coral (DC)	dead coral, dead coral algae, and rubble
Biotic (B)	soft coral, sponge, and fleshy weed
Abiotic (A)	sand, silt, and rock
Others	giant clam, *Acanthaster planci*, *Diadema spp*. etc.

Table 3 Coral cover (%) as a guidance of categorization defined by Gomez and Yap (1988)

Coral cover (%)	Criterion
0.0 – 24.9	Bad
25.0 – 49.9	Moderate
50.0 – 74.9	Good
75.0 – 100.0	Excellent

Table 4 Description of classifications. Visually, the coral reef could be sorted into 2 categories (live and dead coral) according to their color. The live coral is generally found far from land, close to the deep water zone, while dead coral is commonly distributed close to the shoreline (COREMAP 2001, cited in Suwargana 2014)

Classes	Description
Sea water	Purple to blue
Live corals	Cyan to light green
Dead corals	Green with clear boundary
Sea-grasses	Yellow to red (orange) with unclear boundary
Sand	Yellow and red

Table 5 Example of the confusion matrix calculation (from Congalton and Green 2008)

	Field observation (j)			Total N_{i+}
Image	N_{11}	N_{12}	N_{1k}	N_{1+}
Classification	N_{21}	N_{22}	N_{2k}	N_{2+}
(i)	N_{k1}	N_{k2}	N_{kk}	N_{k+}
Total N_{j+}	N_{+1}	N_{+2}	N_{+k}	N

Table 6 Status of coral reefs in study site based on the result of PIT method at 23 transects in 10 islands

Location (ID)	Transect no.	Latitude; Longitude	Depth (m)	% Coral cover	Status
Saugi (SG)	SG.1	4º 45' 57.87″ S; 119º 27' 50.39″ E	3	2	Bad
	SG.2	4º 46' 2.36″ S; 119º 27' 35.47″ E	3	28	Moderate
	SG.3	4º 46' 45.46″ S; 119º 27' 44.12″ E	3	39	Moderate
Samatellu Lompo (SL)	SL.1	4º 42' 13.07″ S; 119º 19' 40.99″ E	3	9	Bad
	SL.2	4º 42' 18.21″ S;: 119º 19' 50.60″ E	3	24	Bad
	SL.3	4º 42' 26.49″ S; 119º 19' 34.74″ E	10	53	Good
Gondongbali (GB)	GB.1	4º 43' 13.72″ S; 119º 3' 42.87″ E	3	54	Good
	GB.2	4º 42' 42.55″ S; 119º 4' 23.11″ E	10	56	Good
Tambakulu (TK)	TK.1	4º 44' 4.14″ S; 119º 3' 46.62″ E	3	2	Bad
	TK.2	4º 44' 40.67″ S; 119º 3' 42.83″ E	10	51	Good
Pandangan (PD)	PD.1	4º 43' 26.50″ S; 118º 59' 5.50″ E	3	6	Bad
	PD.2	4º 43' 11.66″ S; 118º 58' 29.04″ E	10	15	Bad
Kapoposang (KP)	KP.1	4º 41' 51.94″ S; 118º 57' 48.71″ E	3	19	Bad

	KP.2	4º 42' 0.81″ S; 118º 56' 9.06″ E	10	14	Bad
Karanrang (KR)	KR.1	4º 51' 16.71″ S; 119º 23' 3.26″ E	3	18	Bad
	KR.2	4º 51' 16.69″ S; 119º 22' 36.35″ E	3	16	Bad
	KR.3	4º 51' 34.04″ S; 119º 23' 6.64″ E	10	21	Bad
Sarappo Lompo (SR)	SR.1	4º 52' 37.32″ S; 119º 15' 55.19″ E	3	10	Bad
	SR.2	4º 53' 3.78″ S; 119º 16' 5.90″ E	10	56	Good
Sanane (SN)	SN.1	4º 56' 38″ S; 119º 20' 27.50″ E	3	20	Bad
	SN.2	4º 57' 1.83″ S; 119º 20' 20.12″ E	10	7	Bad
Badi (BD)	BD.1	4º 57' 58.16″ S; 119º 17' 11.82″ E	3	16	Bad
	BD.2	4º 58' 16.89″ S; 119º 17' 2.96″ E	10	7	Bad

Table 7 Distance of fishing locations from the mainland (before and in 2014) in the study site. The number in columns of "Before 2014" and "In 2014" were the number of fisherman who chose favorite locations for fishing in the period of before 2014 and in 2014, respectively.

No.	Fishing location	Distance (km)	Before 2014 (The number of person /yr)	In 2014 (The number of person /yr)
1.	Near mainland	3.24	4	10
2.	P. Saugi	6.83	20	18
3.	P. Laiyya	8.87	3	2
4.	P. Karanrang[1,2]	13.54	7	6
5.	P. Salemo	14.52	4	2
6.	P. Lamputang	17.64	4	2
7.	P. Palla	18.66	0	2
8.	P. Pangkaiya	18.85	6	2
9.	P. Podang-podang Caddi	19.40	5	5
10.	P. Samatellu Lompo	22.51	0	4
11.	P. Sanane[1,2]	22.88	6	5
12.	P. Bontosua[1]	23.39	12	4
13.	P. Sarappokeke[1]	26.66	14	6
14.	P. Sarappo[1,2]	26.81	28	32
15.	P. Reangreang[1]	27.27	9	8
16.	P. Badi[1,2]	29.00	8	6
17.	P. Lumulumu[1,2]	36.47	23	23
18.	Gs. Bonebatang[1]	39.37	11	5
19.	P. Kodingareng Keke[2]	41.14	10	7
20.	P. Jangang jangangang[1,2]	41.84	19	24
21.	P. Suranti[1,2]	43.99	24	31
22.	P. Pamanggangang[1,2]	44.50	21	15
23.	P. Tambakulu[1,2]	49.29	26	15
24.	P. Gondongbali[1,2]	49.57	42	40

25.	P. Lanyukang[1,2]	50.33	28	31
26.	P. Langkai[1,2]	50.81	36	42
27.	P. Pandangan[1,2]	58.62	18	11
28.	P. Kapoposang[1,2]	61.22	45	57

[1] Blast fishing

[2] Cyanide fishing

Table 8 Results of the classification of coral reefs and seabed habitats estimated by the multi-temporal Landsat imagery data in the PANGKEP Regency, Spermonde Archipelago, Indonesia

Class	Landsat 8 OLI, 2014			Landsat 7 ETM, 2002			Landsat 5 TM, 1994			Total		
	Areas (ha)	Amount of pixel	%	Areas (ha)	Amount of pixel	%	Areas (ha)	Amount of pixel	%	Area (ha)	Amount of Pixel	%
Live corals	4,236.31	47,071	39.36	6,885.14	76,501	63.96	7,715.67	85,729	71.68	18,837.12	209,301	58.33
Dead corals	4,316.30	47,958	40.09	2,210.04	24,556	20.53	1,128.17	12,535	10.48	7,654.51	85,049	23.7
Sea-grasses	906.08	10,067	8.42	846.09	9,400	7.86	655.89	7,287	6.09	2,408.06	26,754	7.46
Sand	1,305.90	14,510	12.13	823.32	9,148	7.65	1,264.86	14,054	11.75	3,394.08	37,712	10.51
Total	10,764.59	119,605	100.00	10,764.59	119,605	100.00	10,764.59	119,605	100.00	32,293.77	358,815	100.00

Table 9 Confusion matrix value on the classification of four classes of the seabed habitats in the PANGKEP Regency, Spermonde Archipelago, Indonesia

Field data	Field data				Row total
	Live corals	Dead corals	Sea-grasses	Sand	
Live corals	52	8	0	4	64
Dead corals	9	58	0	2	69
Sea-grasses	2	0	40	8	50
Sand	3	0	9	48	60
Column total	66	66	49	62	243

Ta**ble 10** Producer and user accuracy values on the classification of four classes of the seabed habitats in the PANGKEP Regency, Spermonde Archipelago, Indonesia

Producer accuracy (%)			User accuracy (%)		
Field data	Accuracy		Image Classification	Accuracy	
Live corals	52/66	78.78	Live corals	52/64	81.25
Dead corals	58/66	87.87	Dead corals	58/69	84.05
Sea-grasses	40/49	81.63	Sea-grasses	40/50	80.00
Sand	48/62	77.41	Sand	48/60	80.00

Table 11 Change in the area of coral reefs from 1994 to 2014 in the PANGKEP Regency, Spermonde Archipelago, Indonesia. The change of area in each class was established based on the overlay of coral reef distribution and condition map derived from Landsat 5 TM (1994), Landsat 7 ETM (2002), and Landsat 8 OLI (2014) images

Classes	Change in the area (ha)	Ratio (%)
From 1994 to 2002:		
Live corals	-831	-10
Dead corals	882	78.8
Sea-grasses	8	1.0
Sand	-59	-5.5
From 2002 to 2014:		
Live corals	-2,649	-38.5
Dead corals	2,306	114.7
Sea-grasses	60	7.1
Sand	283	27.7

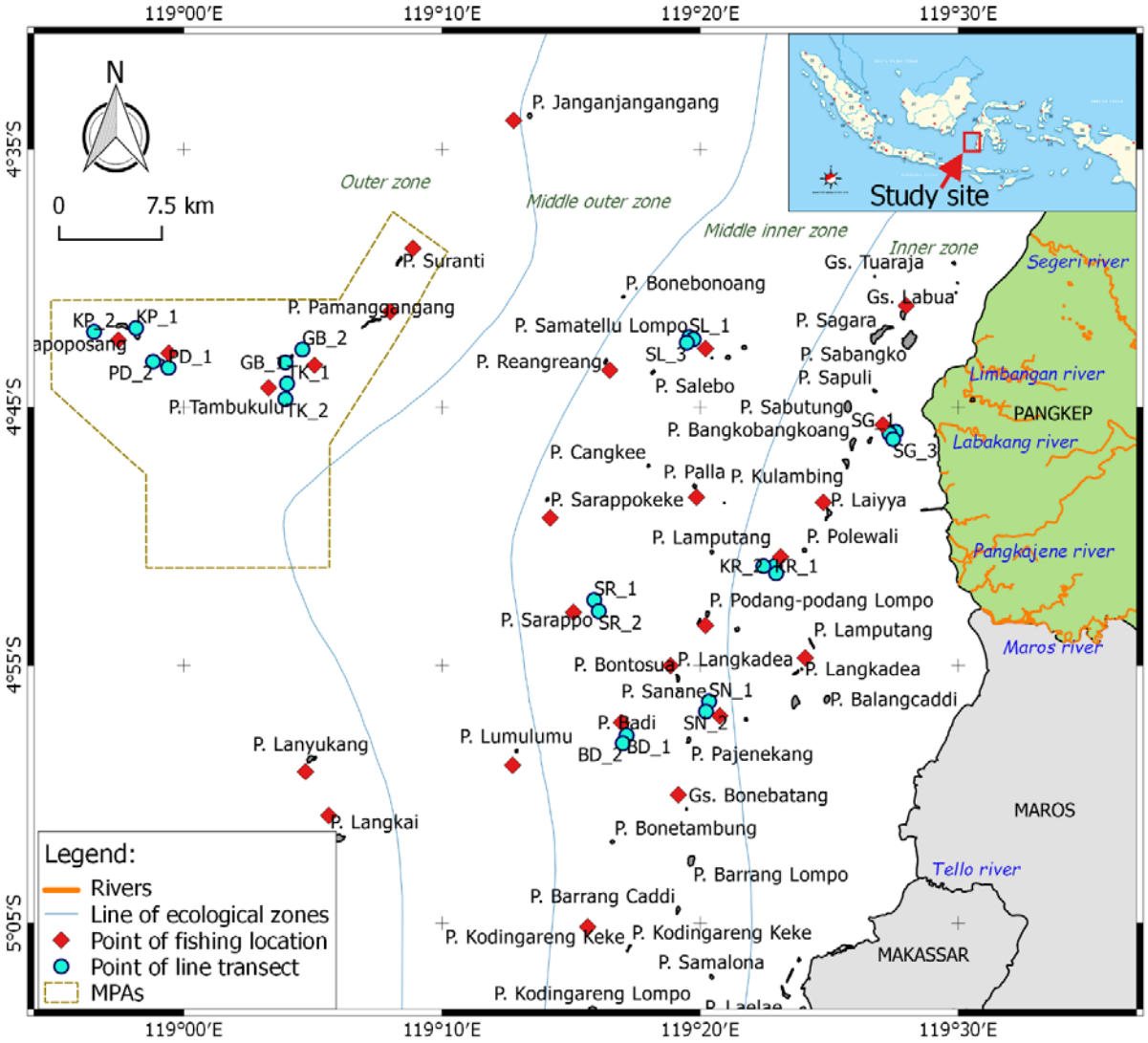

Fig. 1 Map of study area in the PANGKEP Regency, Spermonde Archipelago, South Sulawesi Province, Indonesia

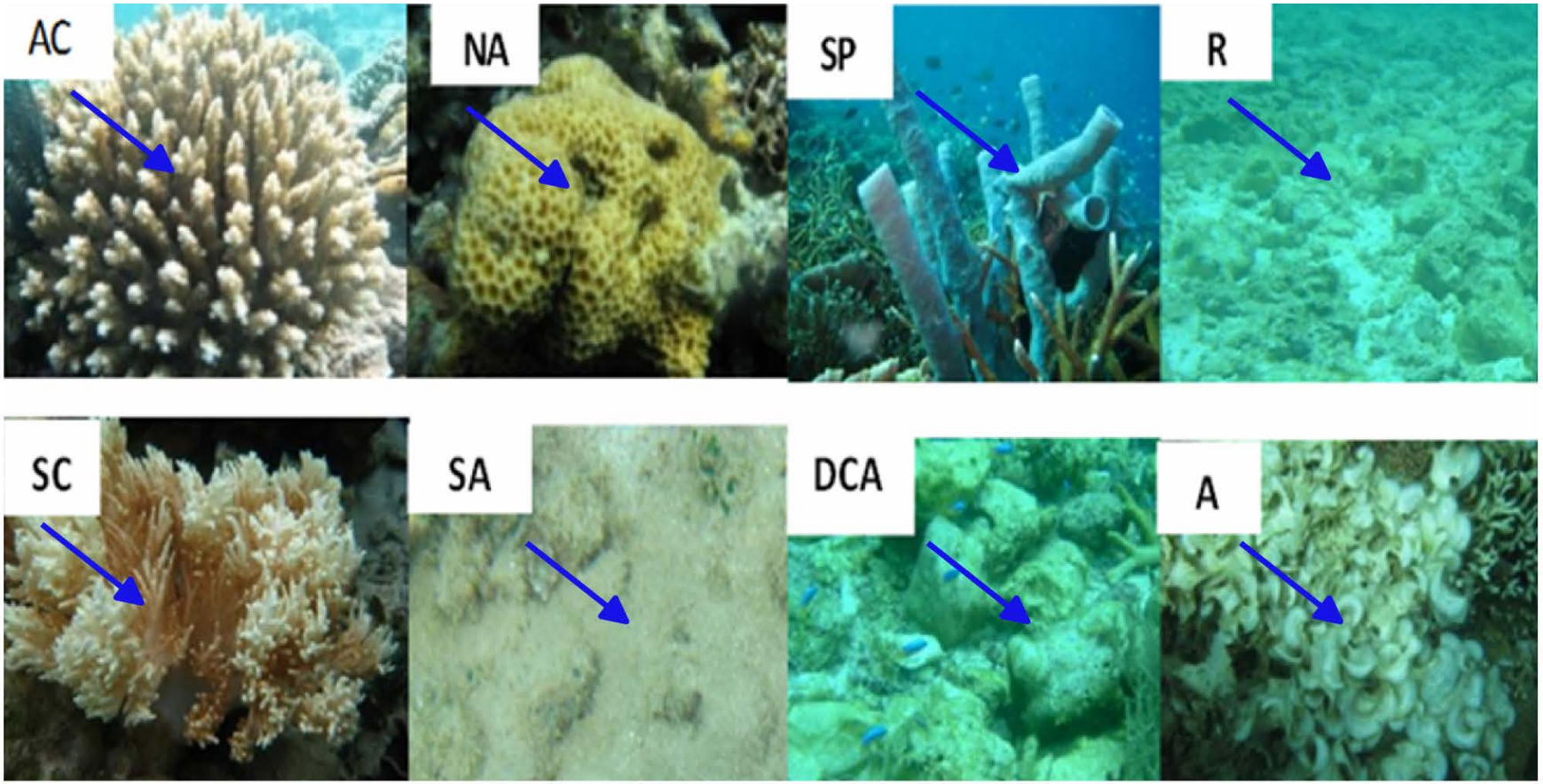

Fig. 2 Categories used in PIT method. AC: Acropora; NA: Non-Acropora; SP: Sponge; R: Rubble; SC: Soft coral; SA: Sand; DCA: Dead coral algae; A: Abiotic.

In this case, the rubble was classified as dead corals

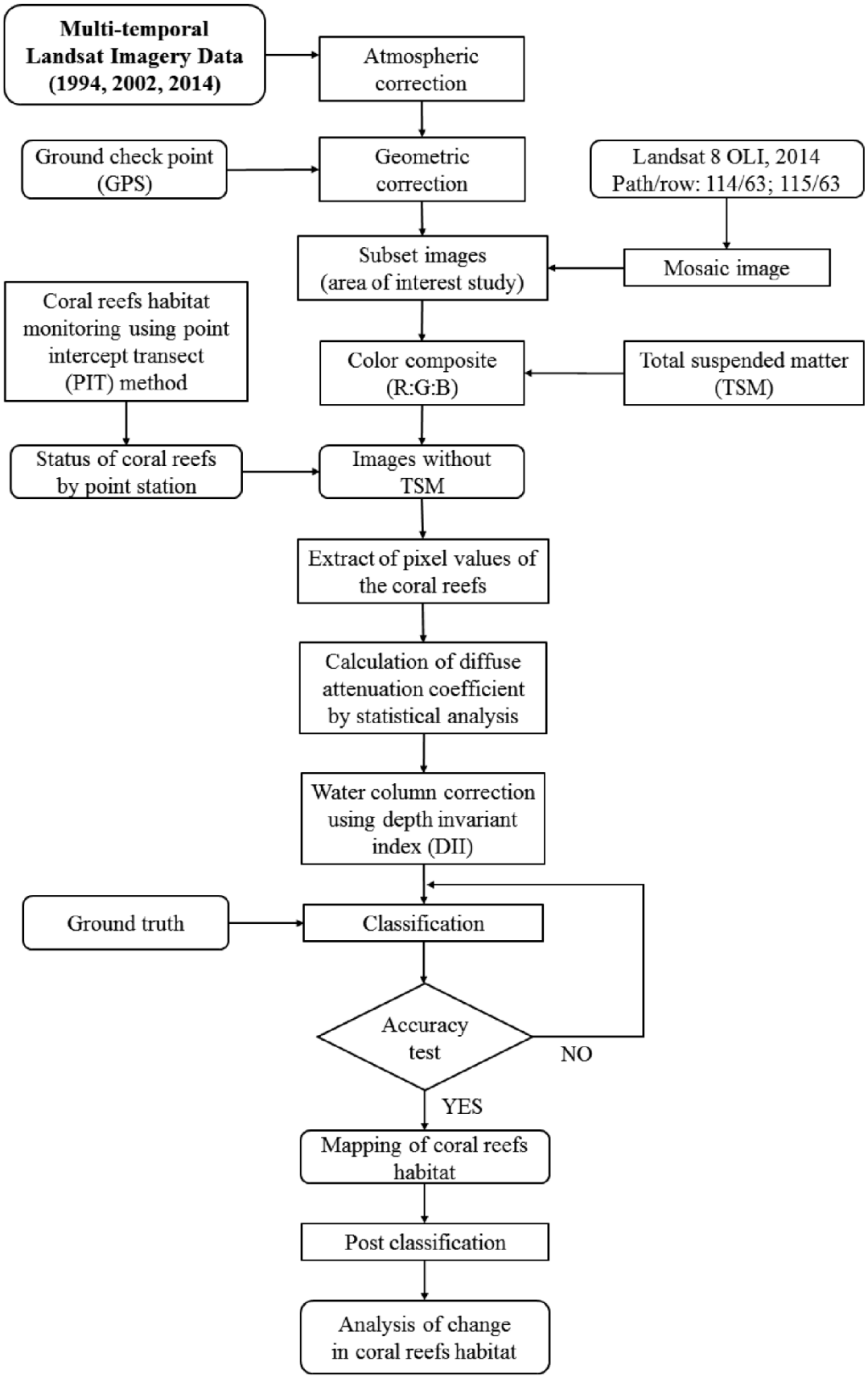

Fig. 3 Flowchart research on mapping and analysis of changes in coral reef habitat

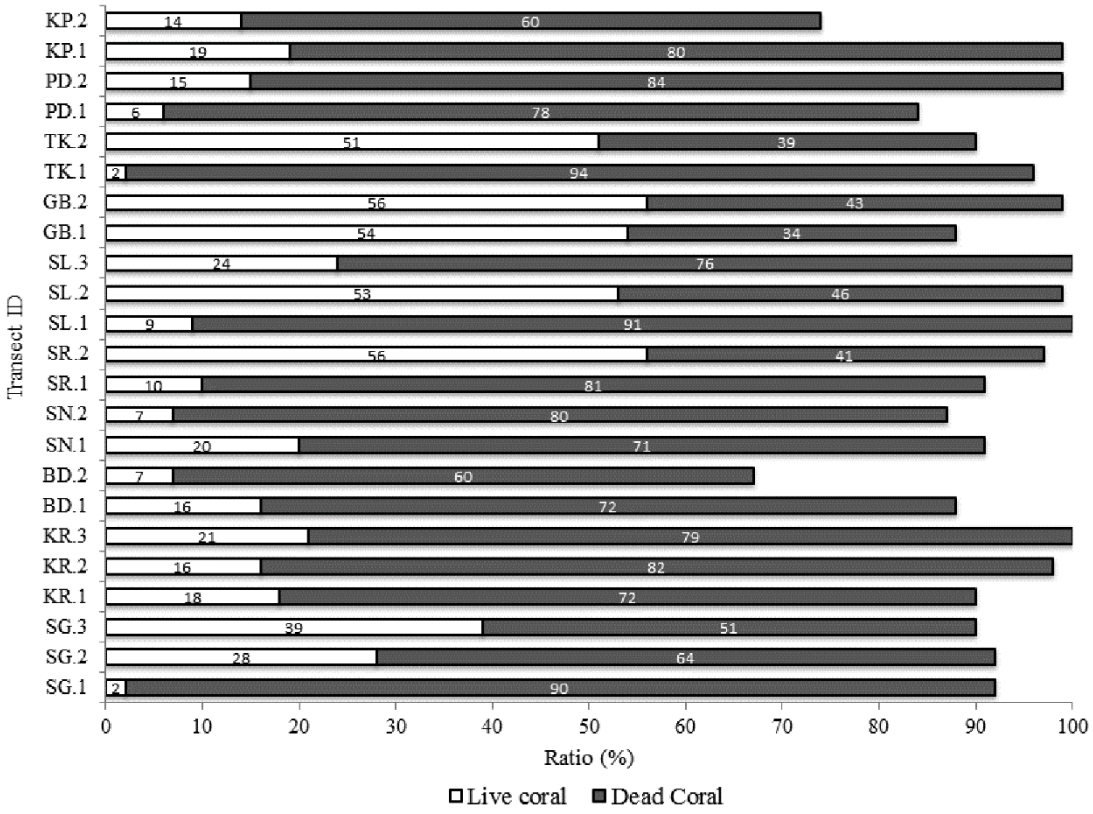

Fig. 4 Ratio of live corals and dead corals at all sites in the PANGKEP Regency, Spermonde Archipelago, Indonesia. The graph summarizes the calculation for each category obtained by PIT method in each village (2-3 observation transects per village)

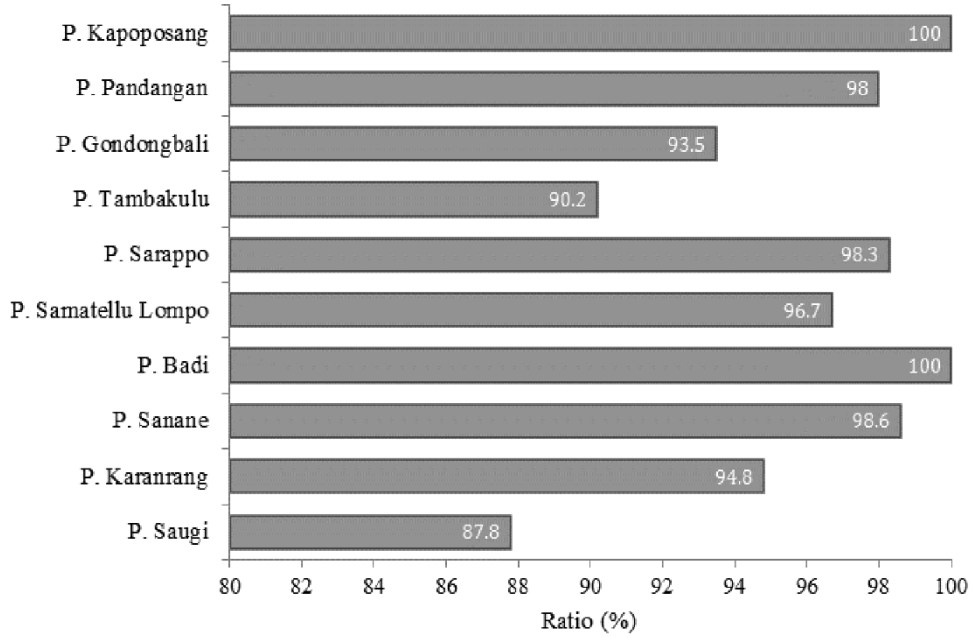

Fig. 5 Averaged ratio of coral rubbles to total dead corals in the PANGKEP Regency, Spermonde Archipelago, Indonesia

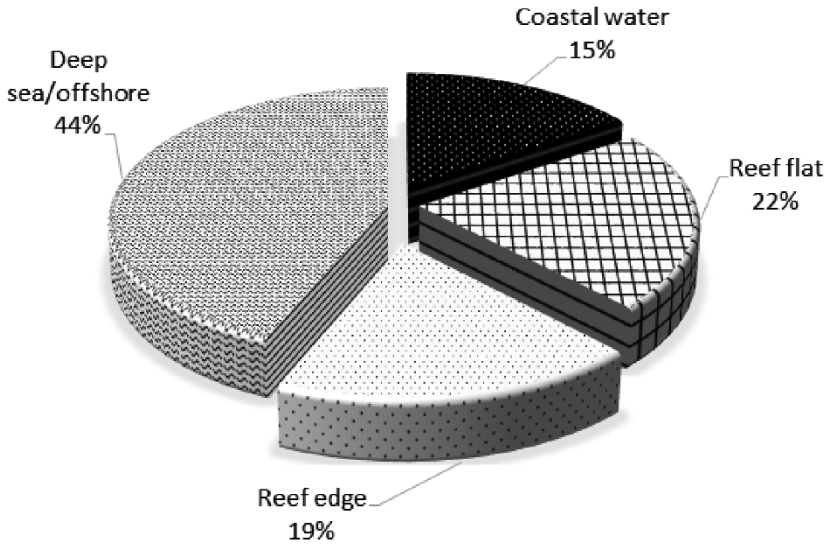

Fig. 6 Ratio of preferred destructive fishing areas (%) obtained by analyzing the results of questionnaires distributed to 296 respondents, which were strongly linked to the fishing gears used and target fish species frequently caught

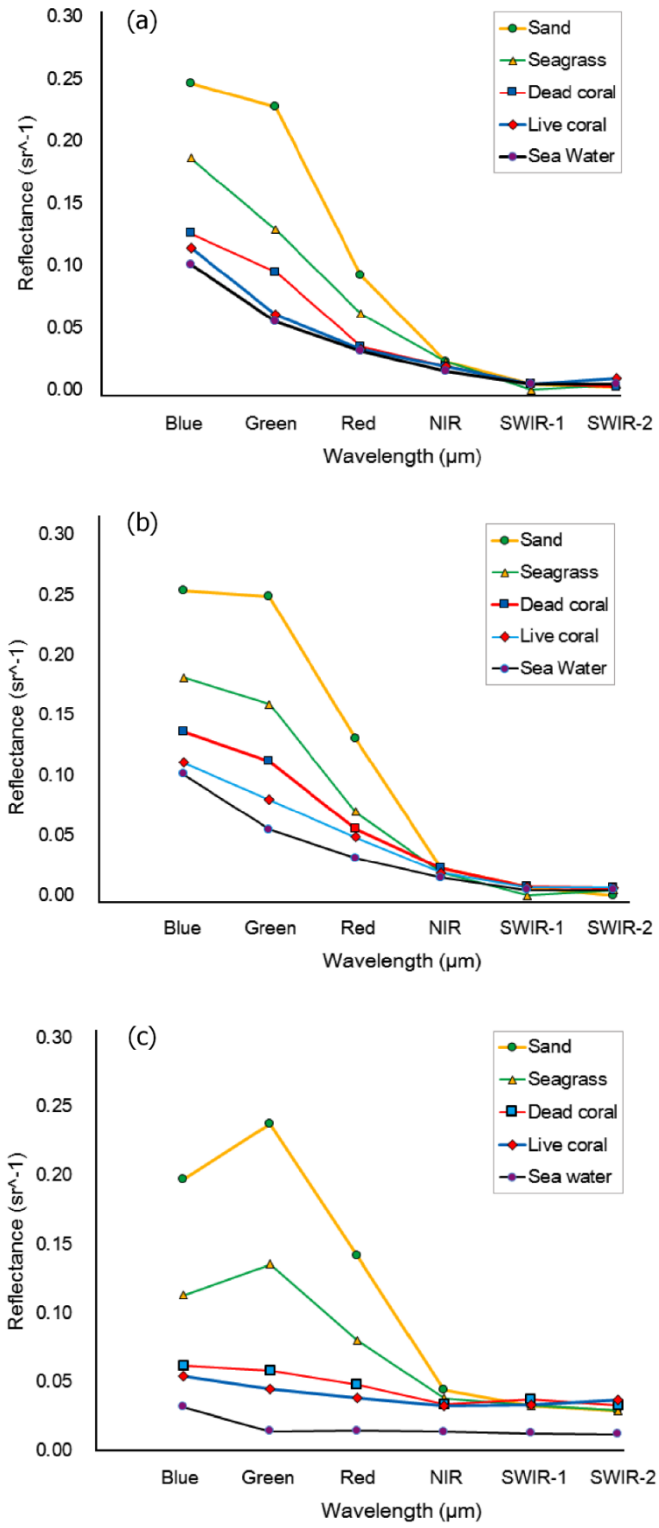

Fig.7 Spectral profile of object classes (sand, seagrasses, dead corals, live corals and sea water) on three series Landsat Imagery data: (a) Landsat TM 1994, (b) Landsat 7 ETM 2002, and (c) Landsat 8 OLI 2014

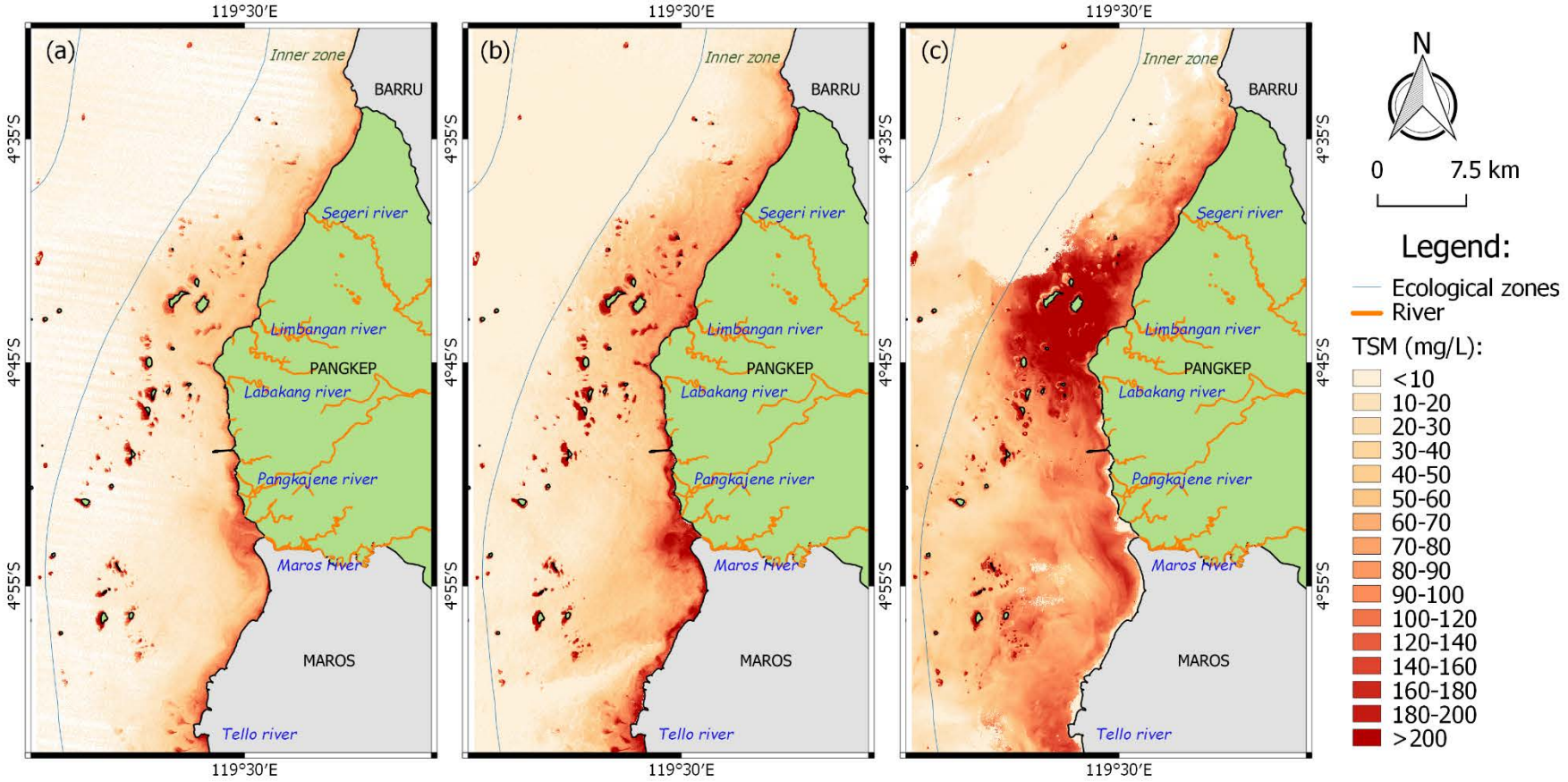

Fig. 8 Distribution and concentration of total suspended matter (TSM) in study area using (a) in Landsat 5 TM, 1994, (b) Landsat 7 ETM, 2002 and (c) Landsat 8 OLI, 2014

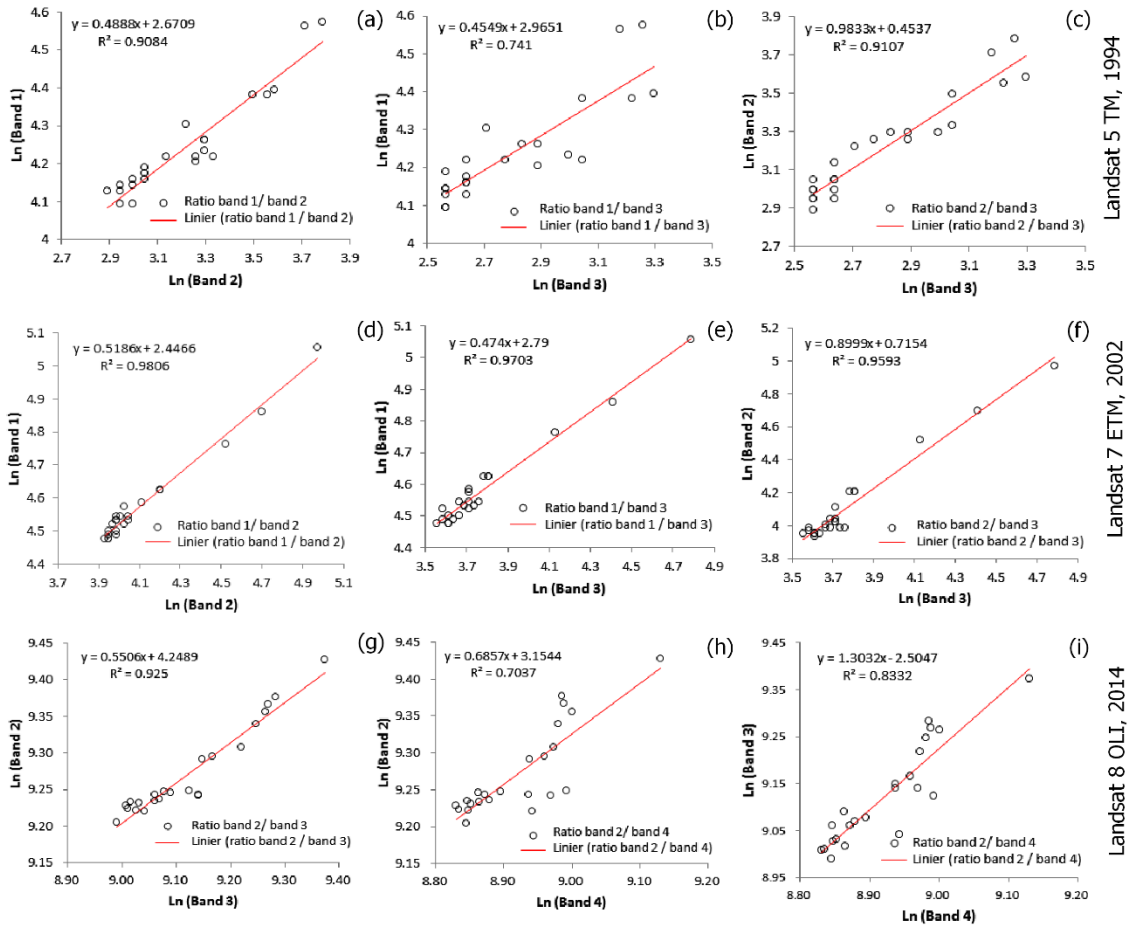

Fig. 9 Plots of spectral values of the coral reef status obtained by three series of multi-temporal Landsat imagery ((a)-(c) for Landsat 5 TM, 1994; (d)-(f) for Landsat 7 ETM, 2002; (g)-(i) for Landsat 8 OLI, 2014) in the PANGKEP Regency, Spermonde Archipelago, Indonesia. (a) and (d): Band 2 vs. Band 3; (b) and (e): Band 1 vs. Band 3, (c), (f) and (g): Band 2 vs. Band 3; (h): Band 2 vs. Band 4; (i) Band 3 vs. Band 4.

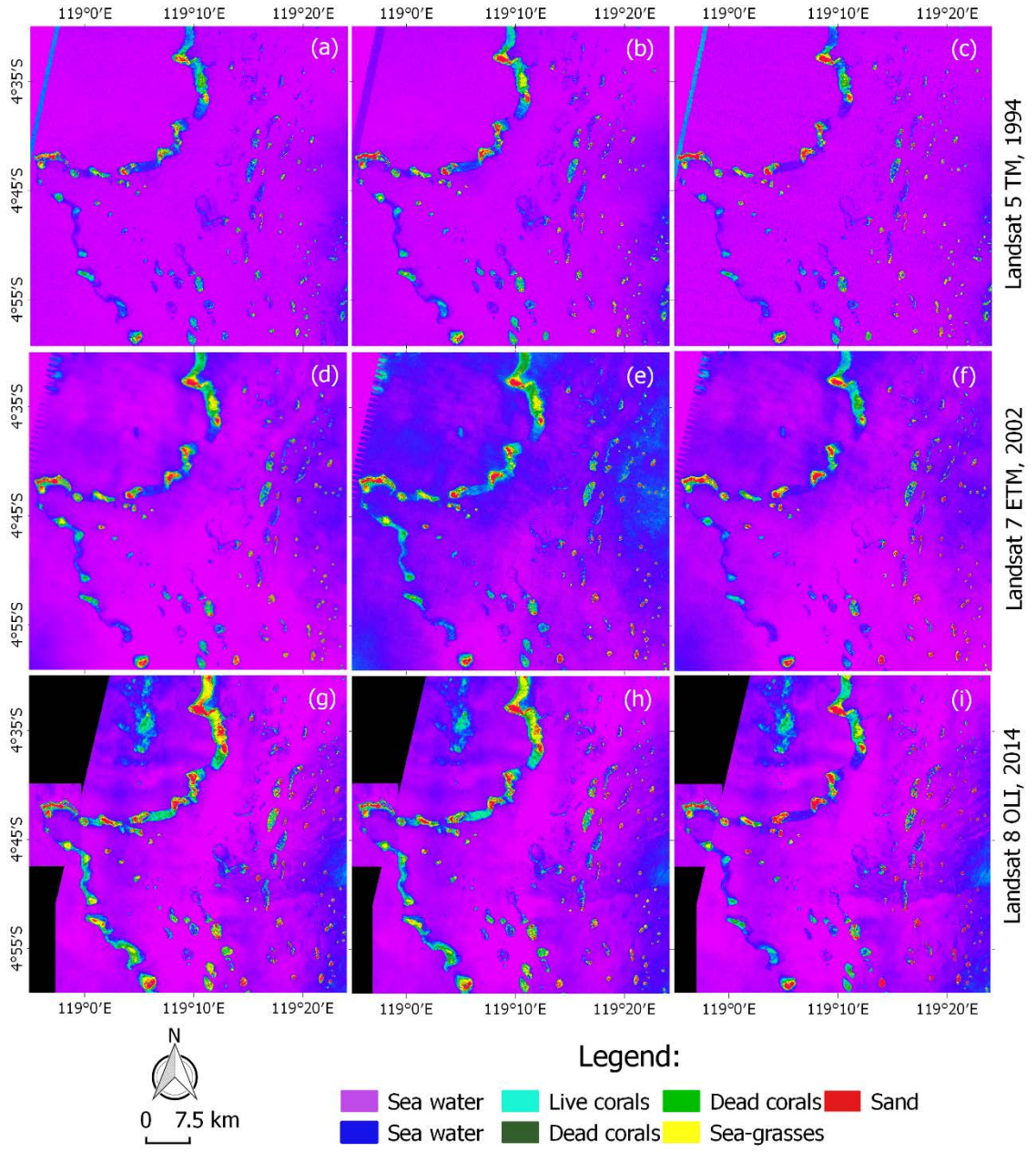

Fig. 10 Depth invariant index derived from three series of multi-temporal Landsat imagery data ((a)-(c) for Landsat 5 TM, 1994; (d)-(f) for Landsat 7 ETM, 2002; (g)-(i) for Landsat 8 OLI, 2014) in the PANGKEP Regency, Spermonde Archipelago, Indonesia, using gradient of the linier line. (a) and (d): Band 2 vs. Band 3; (b) and (e): Band 1 vs. Band 3, (c), (f) and (g): Band 2 vs. Band 3; (h): Band 2 vs. Band 4; (i) Band 3 vs. Band 4.

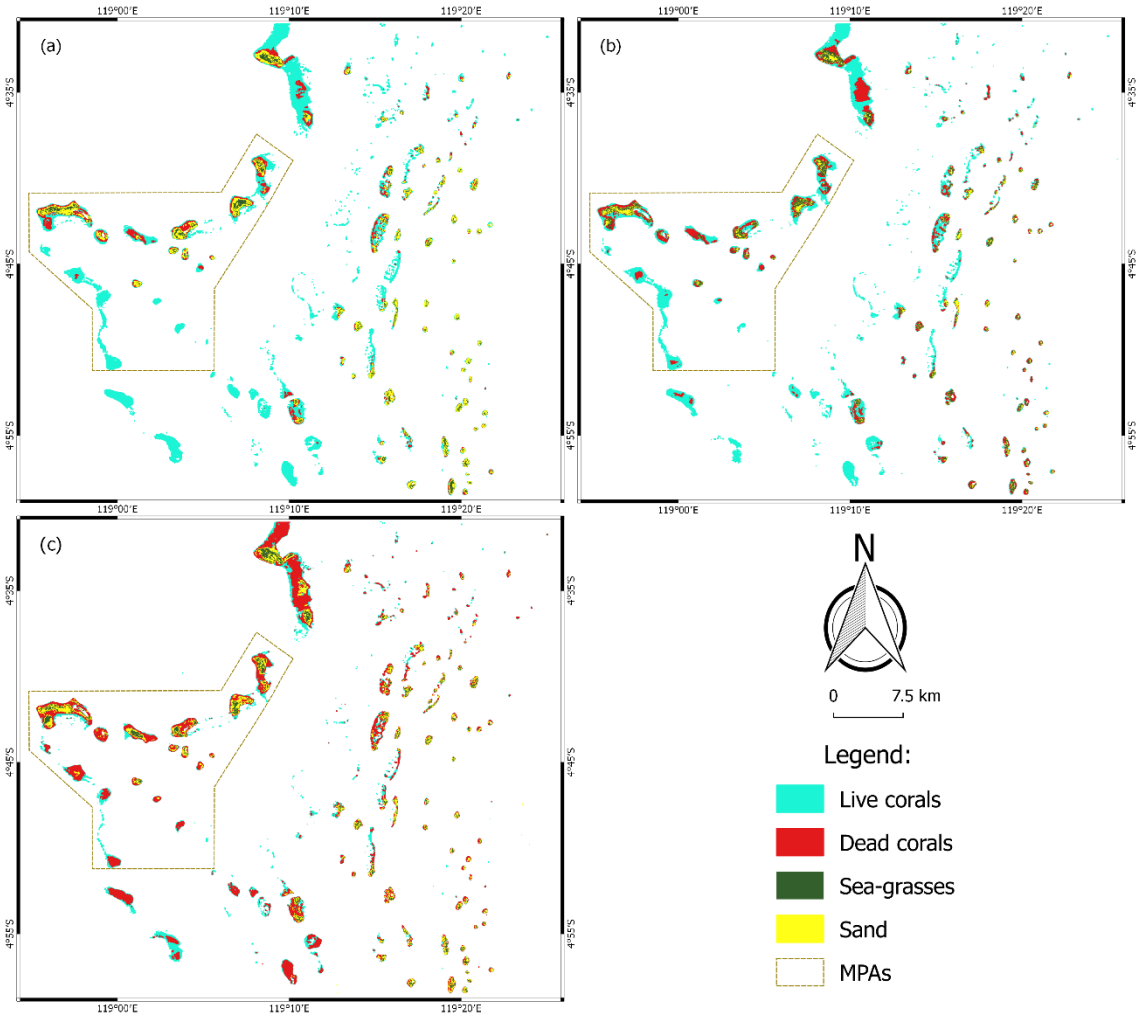

Fig. 11 Distribution and condition of coral reefs in the PANGKEP, Spermonde Archipelago, Indonesia, obtained from three series multi-temporal Landsat imagery data. (a) Landsat 5 TM, 1994; (b) Landsat 7 ETM, 2002; (c) Landsat 8 OLI, 2014

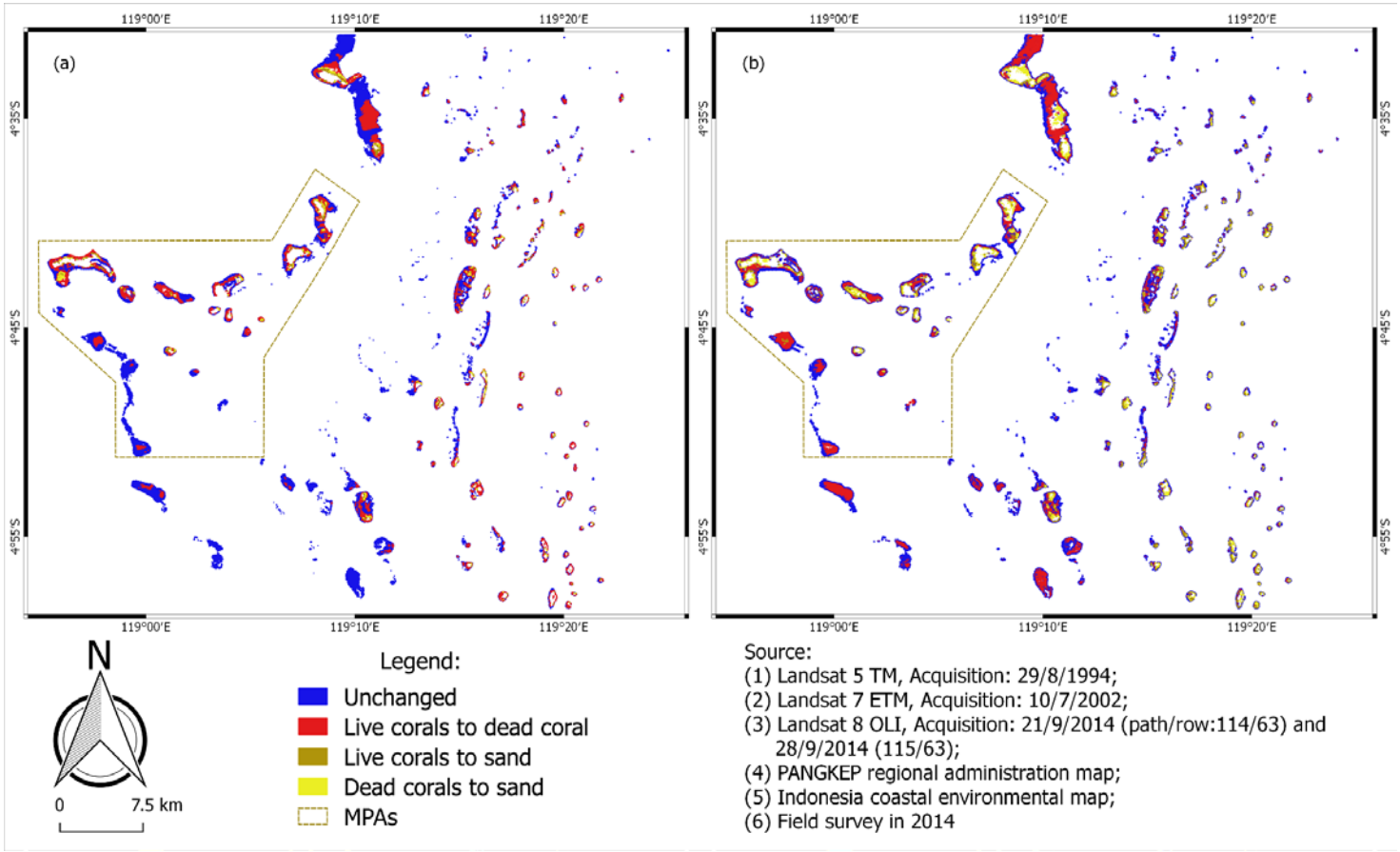

Fig. 12 Map of change in bottom substrate in the PANGKEP Regency, Spermonde Archipelago, Indonesia: (a) from 1994 to 2002 and (b) from 2002 to 2014. The Kapoposang MPAs is located in the outer zone of the PANGKEP islands which also experienced a drastic decline in coral reef habitats in this period

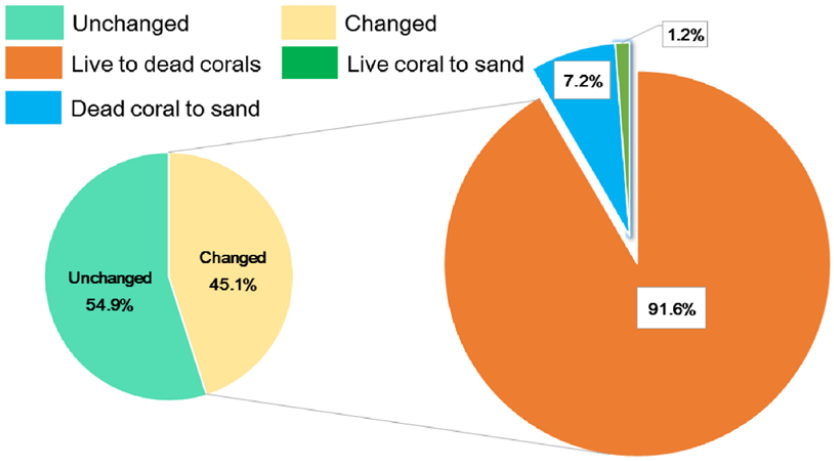

Fig. 13 Change in composition of coral reefs from 1994 to 2014. During the period, 45.1% of the coral reef area was been transformed (left pie chart): 91.6% from live to dead corals, 7.2% from live corals to sand, and 1.2% from dead corals to sand (right pie chart)

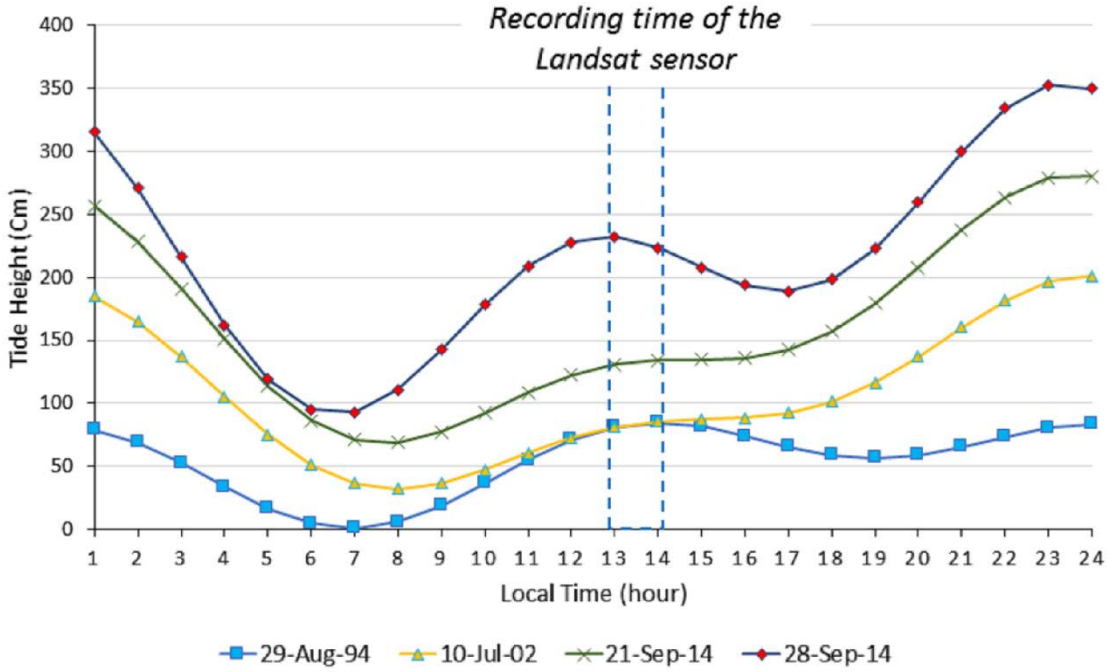

Fig. 14 Tidal prediction in the PANGKEP Regency, Spermonde Archipelago, Indonesia with a coordinate point of observation: 1190 15'36″ S and 40 48'36″ E. The data is processed by using the prediction model from http://www.miz.nao.ac.jp/staffs/nao99/index_En.html. Accessed 10 October 2016